Genesis of chemical sediments in Birimian greenstone belts: evidence from gondites and related manganese-bearing rocks from northern Ghana*

FRANK MELCHER

Institute of Geological Sciences, Mining University, A-8700 Leoben, Austria

Abstract

Early Proterozoic chemical sediments of the Birimian Supergroup in northern Ghana host several types of metamorphosed manganese-bearing rocks. Differences in the mineralogy and geochemistry can be attributed to facies changes in a mixed volcanic–volcaniclastic depositional environment. Manganese oxide-bearing phyllite, which is enriched in transition metals (Cu, Ni, Co, Zn), formed on the flanks of submarine volcanic edifices above an oxidation boundary. Towards the deeper basin, manganese silicate-rich gondites occur. These consist either of spessartine + quartz + ilmenite, or of spessartine + quartz + Mn amphiboles ± rhodonite ± hyalophane ± Mn stilpnomelane ± ilmenite. The Mn amphiboles are identified as manganoan actinolite, tirodite, and dannemorite. Sulphides are widespread as premetamorphic inclusions in Mn garnet grains. In the basin centre, chlorite schist containing garnet with 50–60 mol.% spessartine represents the most distal manganese-bearing rock which is highly diluted by volcanogenic background sedimentation. The origin of Mn-rich rocks is explained by heat-driven seawater convection systems active in submarine volcanic centres that provided hydrothermal solutions. Precipitation of different minerals depended on the geochemical conditions prevailing on the seafloor. During the Eburnean event (around 2000 Ma), the chemical sediments were metamorphosed to upper greenschist or lower amphibolite facies. Mineral assemblages in the gondites point to metamorphic conditions in the range of 450–500°C at 2–3 kbar.

KEYWORDS: gondite, manganese phyllite, hydrothermal activity, Nangodi belt, Lawra belt, Ghana, Birimian Supergroup.

Introduction

MANGANESE-BEARING rocks are important constituents of chemical sediments in many Precambrian supracrustal successions. Oxide-, carbonate-, or silicate-dominated manganese rocks can be differentiated on the basis of predominant manganese-bearing minerals. Gondites are defined as metamorphosed "non-calcareous, manganiferous, arenaceous and argillaceous sediments with spessartine and quartz, commonly with rhodonite and other manganese silicates" (Roy, 1965). They have been reported from a number of Precambrian shields, including India (e.g. Roy, 1968, 1973, 1981; Roy and Purkait, 1968), Guyana (Choubert, 1973), and West Africa (Neumann, 1988). Spessartine–quartz rocks are also known as coticule rocks, for example in Palaeozoic foldbelts of the Ardennes (Kramm, 1976; Krosse and Schreyer, 1993) and the Appalachians (Wonder *et al.*, 1988; Gardiner and Venugopal, 1992). The Proterozoic, metamorphosed massive sulphide deposits of both, Broken Hill (Pb-Zn-Ag), Australia (Spry and Wonder, 1989), and Gamsberg (Zn-Pb), South Africa (Rozendaal and Stumpfl, 1984), are enveloped by manganoan garnet rocks which probably developed from mixing of Mn-rich

* In memory of Dr Alfred Leube (1926–1994).

Mineralogical Magazine, June 1995, Vol. 59, pp. 229–251

hydrothermal emanations and pelagic clays.

In the Birimian (Early Proterozoic) greenstone belts of Ghana, manganese mineralization is widespread (Kesse, 1976), but to date no detailed mineralogical or petrological work has been done on them. One exception is the world-class manganese deposit of Nsuta with reserves of 5 million tonnes of oxide ore containing 48.9 % Mn and 28 million tonnes of carbonate ore assaying 15–30% Mn (Kesse, 1985). There, investigations have focused on the secondary manganese oxide and hydroxide phases (e.g. Sorem and Cameron, 1960; Perseil and Grandin, 1978). The protores are manganese carbonate and silicate rocks containing rhodochrosite, spessartine, and rhodonite. A manganiferous amphibole, tirodite, has been reported from these rocks by Jaffe *et al.* (1961). Carbonaceous phyllite containing an average of 2 wt.% MnO is the most widespread host rock of the Nsuta Mn-bearing succession (Kleinschrot *et al.*, 1993). There is, however, no conclusive genetic concept explaining the origin of the Nsuta protores.

In greenstone belts of northern Ghana, manganese-bearing rocks are associated with chert, epiclastic and tuffaceous rocks, and metavolcanic rocks. Two of these belts were studied in greater detail, and the results of mineralogical and geochemical studies are presented in this paper. The discussion focuses on the implications as to the nature of the initial manganese sediments, the connection to hydrothermal processes, and the metamorphic conditions that can be deduced from the manganese mineral assemblages.

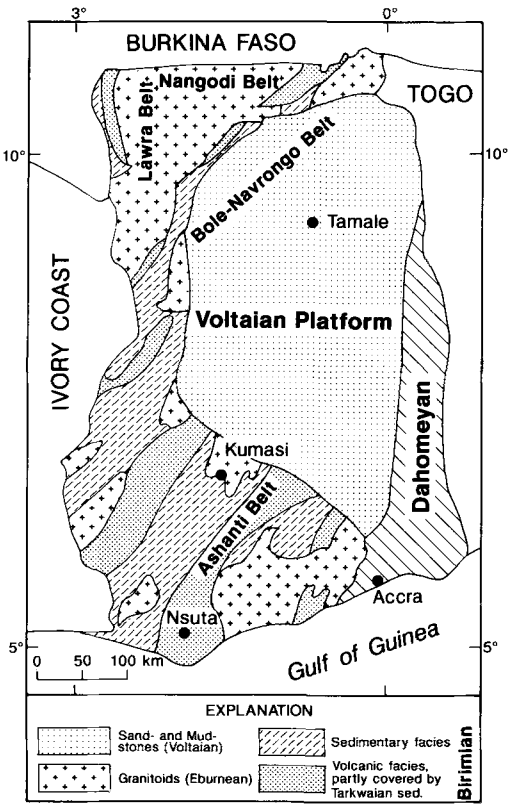

FIG. 1. Simplified geological map of Ghana outlining the Birimian, Dahomeyan and Voltaian systems and indicating the locations of the Nangodi and Lawra belts, and of the Nsuta manganese deposit.

Geologic setting

Early Proterozoic (Birimian) rocks of Ghana are part of the Eburnean province of the Man shield, which is the southern part of the West African craton (Petters, 1991). The Birimian Supergroup (Leube *et al.*, 1990) consists of volcanic, pyroclastic, and sedimentary rocks intruded by various types of granitoids. Volcanic belts of tholeiitic basalt and andesite were deposited between 2200 and 2100 m.y. ago (Abouchami *et al.*, 1990; Taylor *et al.*, 1992), together with pyroclastic material deposited in marine basins. Chemical sediments precipitated contemporaneously on the flanks of volcanic edifices; they consist of manganese-rich rocks, chert, and rocks enriched in carbon, carbonates, or sulphides (Leube *et al.*, 1990). Porphyritic volcanic rocks and granitoids of calc-alkalic affinity may either be coeval with the tholeiitic rocks (Leube *et al.*, 1990; Sylvester and Attoh, 1992) or postdate them (Melcher and Stumpfl, 1992). Parts of the volcanic belts are overlain by clastic strata of the Tarkwaian Group, which was probably deposited in graben structures formed by rifting (Goodwin, 1991). Birimian and Tarkwaian rocks were affected by the Eburnean tectono-thermal event at 2100 to 2000 Ma producing isoclinal folding and metamorphism that reached the greenschist to lower amphibolite facies. The Eburnean event was accompanied by the intrusion of large masses of granitoids into the sedimentary-pyroclastic basins (Hirdes *et al.*, 1992).

In Ghana, six parallel greenstone belts trending north to northeast are recognized. The Nangodi belt in the northern part of the country, which forms part of the extensive Bole-Navrongo greenstone belt (Fig. 1), contains belts of MORB-type metavolcanic rocks which are overlain and intruded by a calc-alkalic volcanic and plutonic assemblage (Melcher and Stumpfl, 1992, 1993). Chemical sediments are present at the boundary between the volcanic belts and basins filled with isoclinally folded metapyroclastic and metasedimentary rocks. The chemical facies consists of manganese-rich rock, chert, ferruginous oolitic chert, phyllitic and epiclastic

rocks enriched in Ba, and various sulphide-bearing, carbonate-bearing, and carbonaceous strata. Lenses of tourmalinite typically occur in the upper parts of tholeiitic pillow basalt sequences. In the Nangodi belt, Birimian volcanic and sedimentary rocks are discordantly overlain by clastic rocks attributed to the Tarkwaian Group. Several types of granitoid rocks in the Nangodi belt, which differ in petrographic and geochemical attributes, prove a complex evolutionary history involving synvolcanic and pre- to syntectonic hornblende-bearing granitoids, late-tectonic hornblende–biotite granitoids, and post-tectonic K-rich granitoids. The latter have been dated at 1968 ± 49 Ma (Leube *et al.*, 1990). The stratigraphic sequence and geologic history of the Lawra belt, in the northwestern corner of Ghana (Fig. 1), are, in principle, similar to the Nangodi belt (Roudakov, 1965; Melcher and Stumpfl, 1992).

Occurrence of manganese-bearing rocks

Manganese-bearing rocks in northern Ghanaian greenstone belts occur as garnet-bearing chlorite schist, manganese oxide-rich phyllite, and manganese silicate-bearing gondite. The latter two are closely associated with tholeiitic volcanic rocks, either as lenses in the upper parts of pillow lavas, or as continuous layers along the boundary between volcanic belts and sedimentary basins (Attoh, 1982). This boundary, known as the transition zone (Leube *et al.*, 1990), hosts rocks of the chemical facies, as well as shear zone-related lode gold deposits (Melcher and Stumpfl, 1993, 1994). Manganese oxide-bearing phyllite and gondite may be intercalated, but typically only one or the other is present in any outcrop. Manganese rocks are closely interstratified with chert, Ba-rich pyroclastic rocks (which rarely bear volcanic pebbles), and carbonaceous phyllite. Manganese-rich rocks typically form elliptical lenses some 30–1000 m in horizontal extent and rising some 10–30 m above the surrounding plain steppe terrain. The transition zone attains a maximum thickness of 50–100 m, with single manganese-rich layers ranging in thickness from several cm to 5 m. Isoclinal folding on a small scale makes estimation of a true thickness difficult. Primary sedimentological features such as graded bedding, channel structures, and slump structures are partly preserved. Gondites are generally more massive in outcrop than the manganese oxide-bearing rocks which show a pronounced slaty cleavage. Garnet-bearing chlorite schist is encountered only in successions of the sedimentary basins and is associated with beds of tuff, phyllite, manganese oxide-bearing phyllite, and some massive andesitic greenstone. Because of competency contrasts between units of massive, nearly unfoliated greenstone and soft, foliated metasedimentary rocks, the transition zone acted as a zone of weakness during the Eburnean orogeny, resulting in small-scale isoclinal and drag folding, and in the development of shear zones parallel to the main cleavage.

Mineralogy of manganese-bearing rocks

Manganese oxide-bearing phyllites

Manganese oxide-bearing phyllite is the most common type of manganese rock and contains the assemblage: manganese oxides and hydroxides, iron hydroxides, rutile, quartz, white mica, and chlorite. Rutile is, in places, pseudomorphous after titanite. Manganese minerals are present as coarse-grained pyrolusite and fine-grained aggregates of greyish minerals of the manganomelane group. These occur in layers of variable thickness (0.1 mm to several cm) that are concordant to bedding and are folded and crenulated together with layers rich in silicates, goethite, or rutile. The dense, massive aggregates or needle-like disseminations of minerals of the manganomelane group are identified by electron microprobe analysis as K-and Ca-bearing 'cryptomelane' (see section Manganese oxides and hydroxides). Textural observations indicate that they do not replace silicate minerals. Pyrolusite generally postdates cryptomelane. The compositions of white micas range from ordinary muscovite (MgO and FeO < 2 wt.%, MnO ± 0.2 wt.%) to phengite (FeO 7–8 wt.%, MgO ± 1 wt.%, MnO ± 0.6 wt.%, BaO ± 0.6 wt.%).

Gondites

Gondites in northern Ghana can be divided into two groups. They are either pure spessartine–quartz rocks, or spessartine–quartz rocks with varying amounts of Mn and Ba silicates. Secondary Mn oxides and hydroxides, Ti oxides, sulphides, and accessories occur in both types (Table 1). Pure spessartine–quartz rocks occur both as lenses hosted by greenstone, and as more extensive layers in sedimentary and pyroclastic successions. The rocks contain minor amounts of ilmenite, pseudorutile or rutile, amphibole and sulphides. Multimineral gondites are banded or massive rocks which commonly occur in thick layers at the boundary between metavolcanics and metapyroclastic/sedimentary rocks.

Garnet. Idiomorphic garnet, of 10–100 μm size, is the most important constituent of gondites, and is second in abundance only to quartz. The garnet occurs as either densely packed with grain boundaries touching other garnet grains, as dense aggregates, and as single, isolated grains. Its

TABLE 1. Mineral assemblages of manganese-bearing rocks from the Nangodi and Lawra belts, northern Ghana. Abbreviations used in the text are given in parentheses

Precursor minerals/ materials	Pre-metamorphic change	Metamorphic minerals	Supergene minerals
1) Mn silicate rock →		Gondite	
Quartz (chert)		Recrystallized quartz	
Mn silicate gels?		Spessartine (Ga)	Cryptomelane
Mn carbonates?		Rhodonite (Rdn)	Pyrolusite
Mn oxides?		Calcic manganoan amphibole* (Cam)	Romanèchite
'Clay'		Tirodite (Tir)*	Goethite
Ilmenite →	Pseudorutile (Psrt)*	Dannemorite (Dan)*	Lepidocrocite
Pyrophanite	Rutile	Manganophyllite (Mph)*	
Apatite		Stilpnomelane (Stilp)*	
Sphene		Parsettensite (Pars)*	
Pyrrhotite		Hyalophane (Hyal)*	
Chalcopyrite →	Covellite	Hollandite(?)	
Pentlandite		Graphite (?)	
Pyrite		Rutile	
Sphalerite			
Cobaltite (?)			
2) Mn oxide rock →		Mn-bearing phyllite	
Quartz		Quartz	Cryptomelane
Ash-fall material ('clay')		Chlorite	Pyrolusite
Mn oxides/hyroxides		Muscovite	Goethite
Fe oxides/hydroxides		Phengite	
Ti oxides		Mn oxides/hydroxides (?)	
		Hematite (?)	
		Rutile	

General formulae of minerals marked with *: Psrt $Fe_2Ti_3O_9$

Cam	$Ca_2(Mg,Mn,Fe)_5(Si_8O_{22})(OH)_2$	Mph	$K(Fe,Mn,Mg)_3(Al,Si)_4O_{10}(OH,F)_2$
Tir/Dan	$(Mn,Mg,Fe)_7(Si_8O_{22})(OH)_2$	Stilp	$(K,Ca,Na)_{0.6}(Fe,Mg,Mn)_6Si_8Al(O,OH)_{27}\cdot 2-4H_2O$
Hyal	$(K,Ba)[Al(Al,Si)Si_2O_8]$	Pars	$(K,Na,Ca)(Mn,Al)_7Si_8O_{20}(OH)_8\cdot 2H_2O$

distribution in some layers resembles sedimentary graded bedding. In outcrops close to shear zones, grains may be extremely elongated, indicating ductile high-temperature deformation. However, the metamorphic mineral growth typically postdates the deformation. Some garnet grains show distinct optical inhomogeneity: inclusion-rich, darker cores (ilmenite, rutile, sulphides, probably also submicroscopic carbonaceous material; Fig. 2*a*) and clear rims probably indicate multi-stage garnet growth. The surrounding matrix is chiefly quartz, but ilmenite, amphiboles or other silicates also occur. Garnet grains in unweathered rocks are fresh, but gradations to garnet pseudomorphs completely replaced by manganese and iron hydroxides can be observed in samples affected by surficial oxidation processes. However, the garnet has been altered less than other matrix minerals. For example a specimen from the Lawra belt shows fresh garnet grains surrounded by a matrix completely replaced by manganese hydroxides (Fig. 2*b*).

The garnets are members of the spessartine–almandine–grossular series, with most compositions plotting near the spessartine end-member (Fig. 3*a*). The maximum MnO content is 37 wt.%, or 90 mol.% spessartine. The average compositions of garnet from the various localitites are shown in Table 2, and some representative analyses are given in Table 3. The MgO contents are very low in all samples (< 1.1 wt.%), and TiO_2 contents are in the range of 0.3–0.4 wt.%. Andradite contents (Fe^{3+} recalculated from microprobe analyses) are generally < 10 mol.% and average 1–3 mol.% in samples from the Nangodi belt, whereas garnets in the Lawra belt are recalculated to 13–14 mol.% andradite. Chemical zoning is only rarely observed, and due to the small grain size, abundant inclusions, and just slight differences in absolute element contents, is difficult

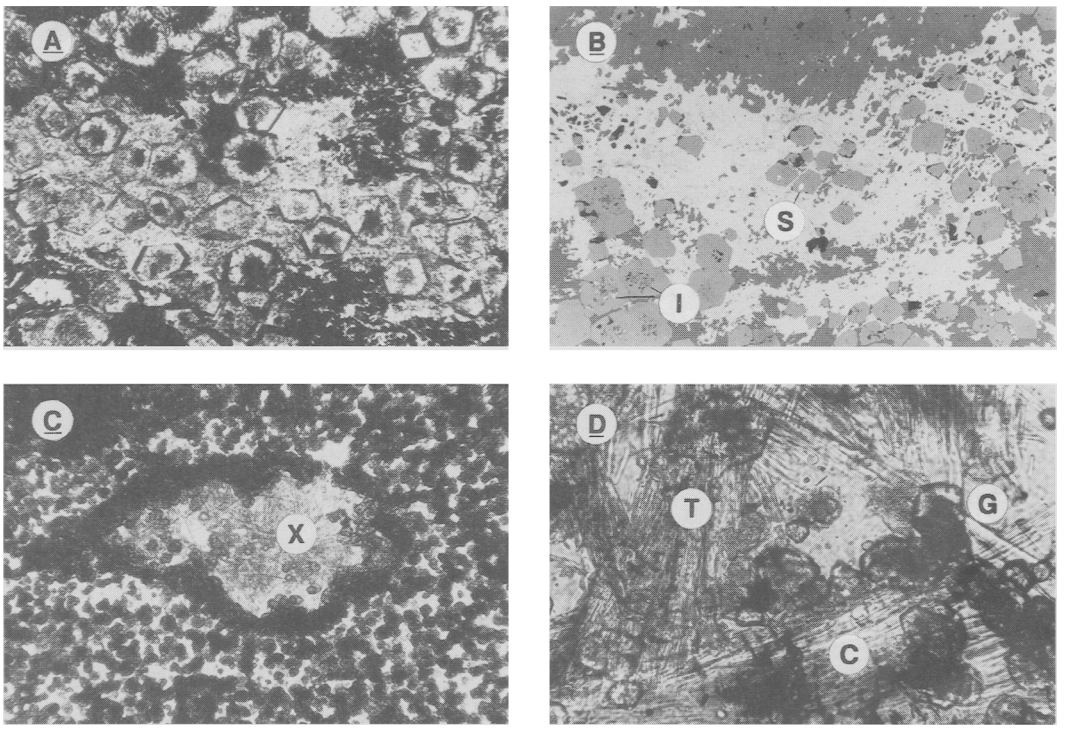

FIG. 2. Photomicrographs of gondites. (A) Idiomorphic, zoned Mn-rich garnets (dark cores: sulphides, ilmenite, carbonaceous matter) embedded in quartz (light) and secondary Mn hydroxides (black). Field of view = 1 mm across. Transmitted light, parallel nicols. Lawra belt (L21). (B) Idiomorphic garnets with inclusions of sulphides (bright white, 'S'), ilmenite (light grey, 'I'), silicates and carbonaceous matter (dark grey), surrounded by secondary cryptomelane (grey) and quartz (black). Field of view = 1 mm across. Reflected light, parallel nicols. Lawra belt (L21). (C) A 'nodule' of Mn amphiboles ('X') surrounded by a rim of dense garnet. Matrix consists of spessartine (dark) and quartz (light). Field of view = 1 mm. Transmitted light, parallel nicols. Nangodi belt (GH 263). (D) Idiomorphic garnets ('G') intergrown with plates of manganoan actinolite ('C'), needles of tirodite ('T'), and quartz. Field of view = 0.4 mm. Transmitted light, parallel nicols. Nangodi belt (GH130).

to interpret. Zoning patterns with cores enriched in Fe (and Ca) and rims enriched in Mn seem to be the most abundant. This may indicate retrograde metamorphic conditions (Neumann, 1988).

Rhodonite is the prominent pyroxenoid mineral in gondites of the Nangodi belt and typically occurs in massive, almost monomineralic layers, 5–10 mm thick, accompanied by small amounts of amphibole, spessartine and quartz. Microprobe analyses reveal a relatively impure and variable composition in terms of CaO (2.6–5.6 wt.%), FeO (4.1–6.8 wt.%), MgO (0–5.1 wt.%) and MnO (36.5–44.6 wt.%; Table 3, Fig. 3*b*).

Hyalophane, the Ba-rich K-feldspar, occurs as a matrix mineral between garnet grains in narrow layers and lenses of gondites at the Pelungu locality of the Nangodi belt. It is furthermore associated with amphiboles and manganophyllite, and with Ba-rich manganese oxides. In the quaternary feldspar system, hyalophane is mainly composed of orthoclase (65–79 mol.%) and celsian (17–32 mol.%, corresponding to 8–14 wt.% BaO), and minor amounts of albite (2–7 mol.%) and anorthite (< 0.6 mol.%) (Fig. 3*c*, Table 3). MnO, FeO and MgO were detected in amounts less than 0.2 wt.%, and exceptionally as much as 0.8 wt.%.

Calcic manganoan amphibole. Large plates of pale brownish, pleochroic amphibole (Fig. 2*d*) are associated with garnet, rhodonite, quartz and hyalophane, and typically are surrounded by rims of tirodite. The plates are characterized by an average of 7.4 wt.% MnO (5.7–11 wt.%), MgO > FeO_{tot} > MnO (Fig. 3*d*), low Al_2O_3 (< 2.5 wt.%), CaO between 8.5 and 11 wt.%, and low alkali contents

TABLE 2. Garnet compositions in selected samples from the Nangodi belt (N) and Lawra belt (L). Arithmetic mean and standard deviation of n analyses are given in mol.%

Sample	Spessartine	Almandine	Grossular	Pyrope	Andradite
Gondites (Spess+Qz)					
N 076 (n = 7)	88 ± 2	0.6 ± 0.6	7.6 ± 2.0	0.0 ± 0.0	4.7 ± 1.5
N 116 (n = 27)	75 ± 4	13.1 ± 3.1	5.2 ± 2.8	2.1 ± 0.7	4.0 ± 2.4
Gondites (Spess+Qz+Amp ± Rdn ± Hyal)					
N 012 (n = 14)	79 ± 3	6.9 ± 1.9	6.7 ± 2.6	2.4 ± 1.1	4.5 ± 1.9
N 130 (n = 22)	78 ± 6	6.2 ± 2.5	9.5 ± 6.1	1.0 ± 0.3	4.9 ± 2.3
N 135 (n = 6)	78 ± 6	10.2 ± 0.3	6.7 ± 0.6	1.5 ± 0.1	3.9 ± 1.8
N 165 (n = 4)	81 ± 3	7.5 ± 2.9	5.7 ± 4.7	0.6 ± 0.3	5.5 ± 4.4
L 13 (n = 3)	76 ± 2	8.1 ± 0.9	0.2 ± 0.1	0.8 ± 0.3	13.8 ± 0.5
Garnet-bearing chlorite schists					
N 231 (n = 6)	54 ± 4	24.3 ± 4.4	19.1 ± 4.1	0.6 ± 0.7	1.9 ± 2.4

(max. 0.33 wt.% Na_2O and 0.1 wt.% K_2O). Calculation of microprobe analyses using the program EMP-Amph (Mogessie *et al.*, 1990) reveals 'tremolitic or actinolitic ferri-manganoan hornblende' on the basis of ΣFM = 13 (in each case, total Fe would be Fe^{3+}), or 'manganoan actinolite' on the basis of ΣCa = 15 (Mogessie and Tessadri, 1982). The CaO contents as low as 8.5 wt.% probably indicate a miscibility with tirodite (Fig. 4). Representative analyses are presented in Table 3.

Tirodite. Manganoan cummingtonite is a very common constituent of gondites in the Nangodi belt. It occurs as needle-like minerals as much as 150 μm in length and 10–20 μm wide (Fig. 2*c,d*). Under the microscope it appears as colourless to greenish or yellowish, strongly anisotropic needles, or, rarely, as prisms. Most crystals are not orientated and some occur as radially-shaped masses pointing to syn- and post-tectonic formation. X-ray powder diffraction patterns of whole-rock samples reveal amphibole peaks that can be attributed to 'manganoan cummingtonite' (PDF File 23-302).

Microprobe measurements show that the amounts of Mn, Mg, and Fe vary only slightly (12–18 wt.% MnO, 12–16 wt.% FeO, 12–15 wt.% MgO). CaO contents range between 0.6 and 7.6 wt.% with clusters at 0.7, 2.5 and 4.3 wt.%. Al_2O_3 contents never exceed 1.2 wt.%, and alkali contents are neglegibly low (Table 3). Calculated with EMP-Amph using ΣCa = 15, the minerals are tirodite and Ca-tirodite. These are monoclinic Fe–Mg–Mn amphiboles of the cummingtonite series characterized by $(Ca+Na)_B < 1.34$, Mn ⩾ 0.5 and Mg/$(Mg+Fe^{2+})$ ⩾ 0.5 (Leake, 1978). Tirodites of the Nangodi belt occupy intermediate positions in the Mn–Fe_{tot}–Mg diagram (Fig. 3*d*). Some analyses show Mn cations > 2, which indicates that Mn occupies sites other than the M(4)-site. The high Ca contents in some samples also require the involvement of Mn in the M(1)-M(3)-sites (Fig. 4); according to Ghose and Hexiong (1989), the site preference of Mn^{2+} for the octahedral sites is $M(4) \geqslant M(1) > M(2) > M(3)$. Calculated site occupancies for selected tirodite analyses are given in Table 4.

Dannemorite. In gondites from the Lawra belt, dannemorite, the Fe-rich variety of manganoan cummingtonite, occurs as colourless idiomorphic rhombs and plates. It is characterized by relatively high refractive index, strong birefringence, inclined extinction (angles of 10–15° with respect to the cleavage), and rare twinning. Plates may exceed 5 mm in length, whereas idiomorphic rhombs usually are less than 0.5 mm. The mineral is associated with garnet, quartz and a brownish, fine-grained mineral resembling manganophyllite. Chemically, dannemorite compositions are characterized by Mg/(Mg+Fe) = 0.30–0.45, Mn/(Mn+Mg+Fe) = 0.24–0.26, Al_2O_3 < 0.4 wt.%, and CaO 1–3 wt.% (Fig. 3*d*, Tables 3, 4).

Manganese-bearing hydrous sheet silicates. Small needles of dark brownish, anisotropic minerals occur in some samples associated with garnet, manganese oxides and amphiboles, or in discrete layers between rhodonite and garnet. Exact microprobe measurements are difficult to obtain due to the small dimensions (typically only 1–5 μm thick), replacement by manganese oxide minerals, and fine intergrowth with quartz. A variety of hydrous sheet silicates appears to be present, with compositions ranging from stilpnomelane and mangano-stilpnomelane to a K- and Mn-rich mineral similar to

TABLE 3. Representative electron microprobe analyses of garnet (Ga), rhodonite (Rdn), hyalophane (Hyal), calcic manganoan amphibole (Cam), tirodite, (Tir), and dannemorite (Dan) from gondites (1) and garnet-bearing chlorite schist (2) of the Nangodi (N) and Lawra belts (L), northern Ghana

Mineral	Ga	Ga	Ga	Rdn	Hyal	Cam	Cam	Tir	Tir	Dan
Rock	1 N	1 N	2 N	1 N	1 N	1 N	1 N	1 N	1 N	1 L
(wt.%)										
SiO_2	36.16	36.41	36.58	47.16	56.44	52.55	52.60	52.14	52.42	48.37
TiO_2	0.38	0.24	0.32	0.06	n.a.	0.21	0.10	n.a.	0.05	0.02
Al_2O_3	19.30	19.35	21.55	0.02	20.16	2.50	1.44	0.20	0.27	0.09
FeO	4.61	3.96	12.46	6.83	0.04	10.16	10.80	12.57	13.84	24.10
MnO	34.21	36.73	22.08	38.42	0.02	6.71	7.99	13.76	15.77	13.36
MgO	0.24	0.45	0.38	3.13	0.04	15.21	14.66	14.96	12.29	8.52
CaO	4.59	2.80	6.74	5.39	0.01	10.19	9.45	4.45	3.39	2.29
BaO	n.a.	n.a.	n.a.	n.a.	11.82	n.a.	n.a.	n.a.	n.a.	n.a.
Na_2O	0.02	n.a.	n.a.	n.a.	0.73	0.33	0.20	0.00	0.03	0.05
K_2O	0.04	n.a.	n.a.	n.a.	10.40	0.07	0.08	0.00	0.03	0.00
Total	99.58	99.94	100.12	101.01	99.65	97.93	97.32	98.09	98.09	96.80
Oxygen	12	12	12	3	32	23	23	23	23	23
Si	2.970	2.988	2.952	0.988	11.245	7.622	7.687	7.700	7.887	7.637
Ti	0.024	0.015	0.020	0.001		0.023	0.011		0.009	0.000
Al	1.868	1.871	2.049	0.000	4.735	0.427	0.248	0.035	0.045	0.019
Fe^{3+}	0.149	0.122	0.006			0.177	0.428	0.566	0.152	0.680
Fe^{2+}	0.168	0.150	0.835	0.120	0.006	1.055	0.892	0.986	1.594	2.497
Mn	2.380	2.553	1.510	0.683	0.004	0.825	0.989	1.721	2.080	1.784
Mg	0.030	0.055	0.046	0.098	0.012	3.288	3.193	3.291	2.758	2.002
Ca	0.404	0.247	0.583	0.121	0.002	1.583	1.479	0.701	0.543	0.389
Ba					0.923					
Na	0.003				0.281	0.093	0.057	0.000	0.009	0.009
K	0.004				2.643	0.013	0.015	0.000	0.009	0.000
Total	8.000	8.001	8.001	2.010	19.850	15.106	15.000	15.000	15.014	15.018

Electron microprobe analyses were carried out using ARL-SEMQ microprobes equipped with four wavelength dispersive spectrometers at the Institute of Geosciences, Leoben, and the Institute of Mineralogy and Petrology, Innsbruck, using an accelerating voltage of 15 kV and a beam current of 20 nA. Counting times were 20 s on peaks and 10 s on backgrounds. The following natural mineral standards were used: kaersutite, almandine, plagioclase, rhodonite, biotite and benitoid. Data reduction was done using the program MacQuant Analysis (E. Mersdorf, University of Innsbruck) according to the procedures developed by Bence and Albee (1968). Mineral formulae are calculated using the programs HYPER-FORM (Bjerg *et al.*, 1992) and EMP-Amph (Mogessie *et al.*, 1990). For all amphiboles, $\Sigma Ca = 15$ is used.

manganophyllite. Stilpnomelane, which is abundant in greenschist metamorphic banded iron formation, contains high Fe contents and may also incorporate considerable amounts of Mn; the highest K_2O content reported for stilpnomelane is 3.4 wt.% (Eggleton and Chappell, 1978).

In the Nangodi gondites, Mn- (1–37 wt.% MnO), Fe- (1.4–32 wt.% FeO), and Al- (1.7–8.9 wt.% Al_2O_3) bearing silicates carrying K_2O (< 2 wt.%) are interpreted as members of the stilpnomelane group. Microprobe analyses also reveal low CaO (< 1.5 wt.%), Na_2O (< 0.4 wt.%), and MgO (< 2.6 wt.%). Analyses bearing high MnO contents (13–37 wt.%) may represent parsettensite, the manganese variety of stilpnomelane (Jakob, 1933), or members of a Fe-Mn stilpnomelane series (Table 5).

Minerals containing K_2O between 2 and 10 wt.% carry relatively constant Al_2O_3 (5–6 wt.%), MnO (7–9 wt.%), FeO (13–16 wt.%), and MgO (4–6 wt.%). They resemble manganophyllite, which, however, is reported to have higher Al_2O_3 and MgO contents (Bilgrami, 1956; Sivaprakash, 1980). Manganese-bearing hydrous sheet silicates in the Nangodi samples therefore may represent an

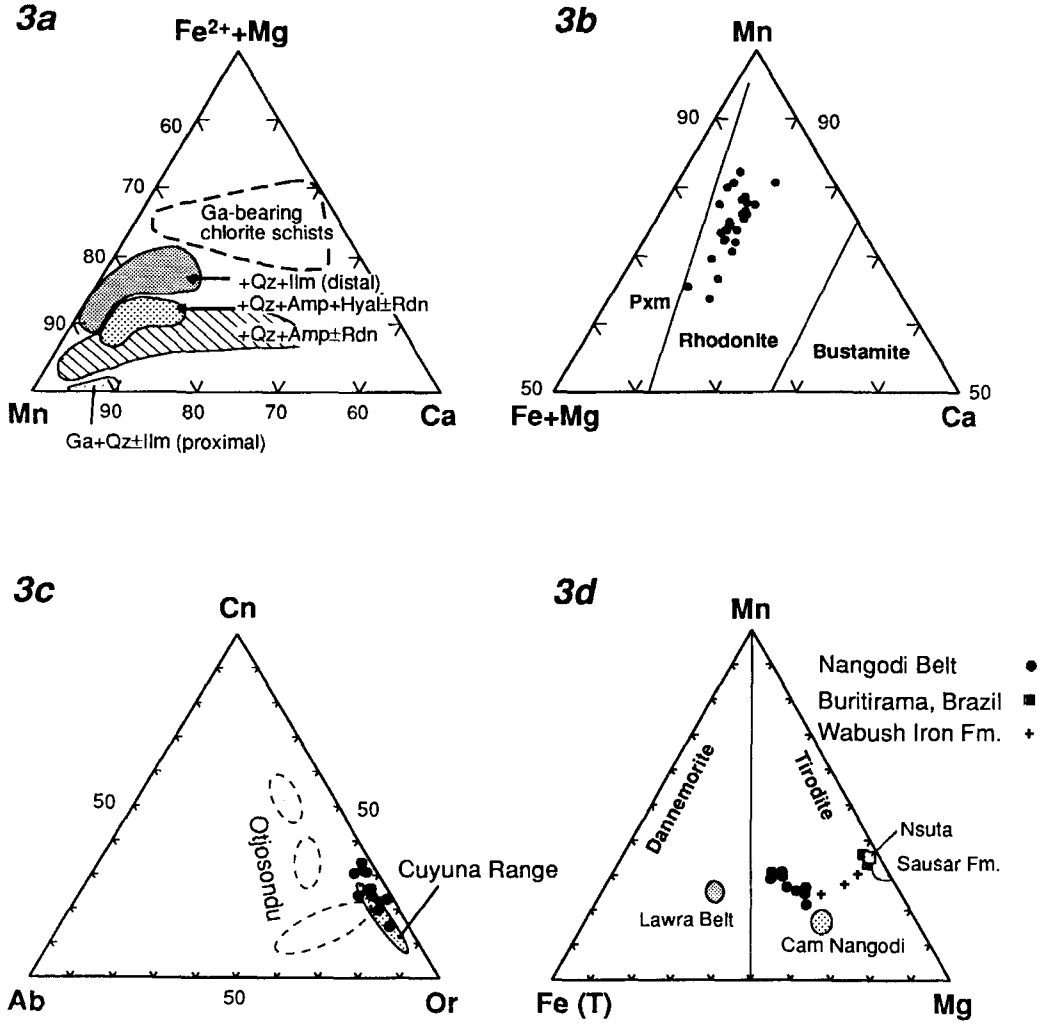

FIG. 3. Triangle diagrams for garnet, rhodonite, hyalophane, and amphibole compositions. (3*a*) Garnet composition in manganese-bearing assemblages of the Nangodi belt. (3*b*) Composition of rhodonite in a diagram according to Winter *et al.* (1981). (3*c*) Composition of Ba-bearing feldspar in the system celsian (Cn)- albite (Ab)- orthoclase (Or). A field for hyalophane from the manganese-rich banded iron formation of the Cuyuna North range, Minnesota (McSwiggen *et al.*, 1994), and three categories of feldspars from the Otjosondu manganese deposit, Namibia (Viswanathan and Kielhorn, 1983), are given for comparison. (3*d*) Amphibole compositions in a diagram Mn–Fe_{tot}–Mg. Literature data obtained from Peters *et al.* (1977, Buritirama), Jaffe *et al.* (1961, Nsuta), Dasgupta *et al.* (1988, Sausar Fm.), and Klein (1964, Wabush Iron Fm.). Amp — amphibole, Ilm — ilmenite, Hyal — hyalophane, Pxm — pyroxmangite, Qz — quartz, Rdn — rhodonite.

evolution series not yet equilibrated from stilpnomelane to manganophyllite.

Pyrophanite, ilmenite and alteration products. Very small, idiomorphic grains of pyrophanite occur in domains rich in quartz and are associated with spessartine and 'stilpnomelane'. Pyrophanite has an ilmenite-type structure; in the reported assemblage, miscibility with geikielite ($MgTiO_3$), ilmenite ($FeTiO_3$) or hematite (Fe_2O_3) components is limited (Table 5). Pyrophanite occurs in some metamorphosed manganese deposits (Sivaprakash, 1980), e.g. as an intergrowth with hematite in the

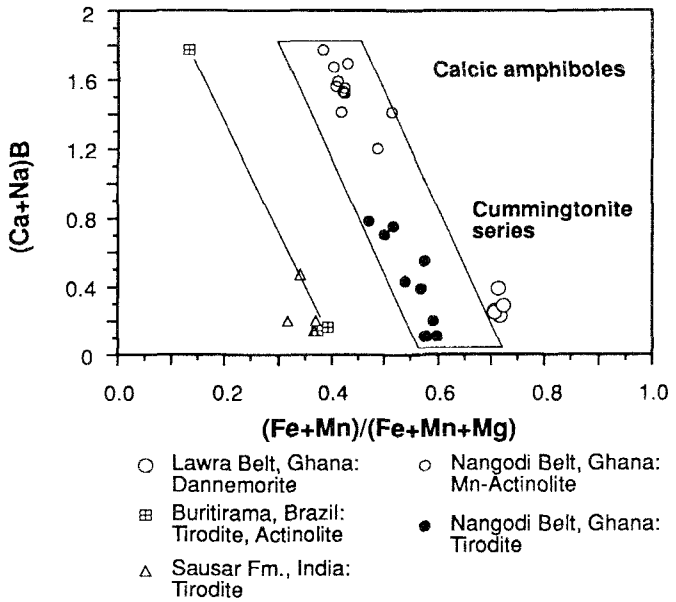

FIG. 4. Plot of Na+Ca in $M(4)$ *vs.* (Fe+Mn)/(Fe+Mn+Mg) for calcic amphiboles and monoclinic Fe–Mg–Mn amphiboles after Robinson *et al.* (1982). Literature data obtained from Peters *et al.* (1977, Buritirama), and Dasgupta *et al.* (1988, Sausar Fm.).

gondites of Chikla, India (Dasgupta *et al.*, 1984). Mn-rich ilmenite with pyrophanite component reaching 62 mol.% is recorded from northern Nigerian manganese occurrences (Neumann, 1988).

Gondites typically contain ilmenite in the matrix and as inclusions in garnet grains (Fig. 2*b*). The tabular, idiomorphic grains are up to 30 μm long and 5–10 μm wide. In reflected light they show a greyish color and abundant internal reflections under crossed nicols. Microprobe analyses show that ilmenite is altered to pseudorutile and hematite. All measured grains are relatively depleted in FeO. MnO contents range from 2.09–4.84 wt.%, corresponding to 4–14 mol.% pyrophanite component in the original ilmenite, assuming MnO was immobile during alteration. This is, however, not necessarily the case (e.g. Melcher, 1991). In Table 5, pseudorutile is recalculated to its theoretical formula $Fe_2Ti_3O_9$; the

TABLE 4. Site occupancies in tirodite (T), Nangodi belt, and dannemorite (D), Lawra belt, calculated to 23 oxygen and ΣCa = 15 (Mogessie *et al.*, 1990)

	T-Site			*M*(1)–*M*(2)–*M*(3)-Site					*M*(4) (B)-Site			
Sample	Si	Al^{IV}	Fe^{3+}	Al^{VI}	Fe^{3+}	Mg	Fe^{2+}	Mn	Mn	Ca	Na	Σ*M*(4)
T 12	7.70	0.04	0.27	–	0.30	3.29	0.99	0.42	1.30	0.70	–	2.00
T 130	7.83	0.17	–	0.05	0.05	3.02	1.57	0.31	1.28	0.71	0.04	2.03
T 130	7.96	0.04	–	0.01	–	3.33	1.62	0.04	1.29	0.68	0.10	2.06
T 130	7.86	0.01	0.14	–	0.14	2.96	1.67	0.24	1.89	0.11	–	2.00
T 130	7.89	0.05	0.07	–	0.08	2.76	1.59	0.65	1.36	0.54	0.01	1.91
T 130	7.99	0.01	–	0.00	–	2.77	2.00	0.24	1.90	0.10	0.01	2.01
T 130	7.72	0.16	0.13	–	0.27	2.82	1.70	0.22	1.79	0.20	–	1.98
D 13	7.64	0.02	0.34	–	0.34	2.00	2.50	0.16	1.62	0.39	0.01	2.02
D 13	7.74	0.02	0.24	–	0.25	2.05	2.70	0.00	1.76	0.25	0.00	2.01

TABLE 5. Representative electron microprobe analyses and calculated formulae of manganophyllite (Mph), parsettensite (Pars), pyrophanite (Pyph), pseudorutile (Psrt), romanèchite (Ro), and cryptomelane (Cpt; M – dense masses, V – veins, N – needles) from gondites (1) and manganese oxide-rich phyllites (2) of the Nangodi belt, northern Ghana

Mineral	Mph	Pars	Pyph	Psrt	Ro	Cpt M	Cpt V	Cpt N
Host rock	1	1	1	1	1	2	1	1
SiO_2	47.35	44.01			1.63	0.35	0.24	0.84
TiO_2	n.a.	0.00	50.95	58.33	n.a.	n.a.	n.a.	n.a.
MnO_2					67.21	81.04	91.12	89.72
Al_2O_3	4.98	2.24	0.28	3.11	1.43	1.53	0.30	0.47
Fe_2O_3				31.40	10.31	1.88	0.31	1.40
FeO	15.18	7.14	2.94					
MnO	7.98	29.16	45.49	3.16				
MgO	5.54	0.35	0.04	0.06	0.19	n.a.	n.a.	n.a.
CaO	0.04	1.16	0.22	0.00	2.52	1.00	0.25	0.00
BaO	0.00	n.a.	n.a.	n.a.	4.60	0.05	0.00	0.27
Na_2O	0.00	0.10	0.00	0.00	0.41	n.a.	n.a.	n.a.
K_2O	9.21	0.52	0.00	0.00	0.48	0.82	2.35	1.14
CoO	n.a.	n.a.	n.a.	n.a.	n.a.	0.33	0.23	0.04
CuO	n.a.	n.a.	n.a.	n.a.	n.a.	0.00	0.64	0.40
NiO	n.a.	n.a.	n.a.	n.a.	n.a.	0.24	0.00	0.11
Total	90.29	84.68	99.92	96.06	88.77	87.28	95.44	94.39
Oxygen	22	22	3	9	16	16	16	16
Si	7.596	7.755			0.225	0.047	0.030	0.104
Ti			0.961	3.004				
Mn^{4+}					6.418	7.490	7.766	7.669
Al	0.942	0.465	0.008	0.251	0.233	0.241	0.044	0.069
Fe^{3+}			0.062	1.618	1.072	0.189	0.029	0.130
Fe^{2+}	2.036	1.052						
Mn^{2+}	1.084	4.352	0.966	0.183				
Mg	1.325	0.092	0.001	0.006	0.039			
Ca	0.007	0.219	0.006	0.000	0.373	0.143	0.033	0.000
Ba	0.000				0.249	0.003	0.000	0.013
Na	0.000	0.034			0.109			
K	1.885	0.117			0.084	0.140	0.370	0.180
Co						0.035	0.023	0.004
Ni						0.026	0.000	0.011
Cu						0.004	0.060	0.037
Total	14.876	14.087	2.004	5.062	8.802	8.318	8.353	8.217

All Mn is assumed to be divalent in Mph, Pars, Pyph and Psrt, and quadrivalent in manganese oxides. All Fe is assumed to be divalent in Mph and Pars, and trivalent in titanium-iron, and manganese oxides. n.a. — not analysed.

low total is caused by structurally involved water. Ti/(Ti + Fe) in all analyses ranges from 0.62 to 0.65, which is in the range of pseudorutile defined by Frost *et al.* (1983). Pseudorutile is intergrown with narrow lamellae and grains of secondary hematite. In most gondites, large amounts of rutile occur in the quartz matrix and as inclusions in garnets. It may have formed from manganoan ilmenite by continuous alteration through pseudorutile to leucoxene, a polycrystalline aggregate of rutile. Because ilmenite enclosed in garnet grains typically has the same degree of alteration as ilmenite in the matrix, the alteration probably predates garnet growth.

Pseudorutile is reported to occur mainly in recent beach sand deposits, originating from alteration of ilmenite in ground water environments, in laterites, and rarely, in lithified rocks (references in Melcher, 1991). Recently, it has been observed in a metamorphosed weathering horizon in the Eastern Alps (Melcher, 1991), and as pre- or synmetamorphic

alteration products of ilmenite in manganese deposits of Nigeria (Mücke and Okujeni, 1984; Neumann, 1988; Mücke and Bhadra Chaudhuri, 1991).

Sulphide minerals. Gondites commonly carry small amounts of sulphide minerals which are partly responsible for elevated base metal contents in these rocks. Sulphide minerals typically occur as inclusions of 2–20 μm size in manganese silicates, especially in garnet, pointing to pre-metamorphic sulphide precipitation. They are commonly enriched as small blebs in garnet cores (Fig. 2*b*). Pyrrhotite, chalcopyrite, pentlandite, pyrite, sphalerite and a Co-bearing mineral (cobaltite?) coexisting with chalcopyrite were identified. Chalcopyrite enclosed in garnet in places is rimmed by covellite indicating pre-metamorphic alteration. In narrow quartz–Mn-oxide veins a bornite–digenite–chalcopyrite–pyrite assemblage occurs. Sandwich-type intergrowths of two or three sulphide minerals in garnet grains point to metamorphic equilibration of the assemblage. The sulphides probably originate from high temperature (> 300°C) monosulphide solid solutions (MSS). Similar inclusions have been observed in garnets from Nigerian gondites (Neumann, 1988).

Manganese oxides and hydroxides. Tetravalent manganese oxides include pyrolusite (β-MnO_2) and minerals of the manganomelane group. Manganomelane minerals are complex low-temperature phases of poor crystallinity, which are not easily identified by reflected light microscopy or electron microprobe analysis. Most of these minerals occur as extremely fine-grained masses or as small needles replacing manganese silicates (garnet, rhodonite, amphibole). The diverse manganomelane group with the general formula $A_{1-2}Mn_8O_{16}{\cdot}xH_2O$ (A = principally Ba, K, Na, Pb; Mn as Mn^{4+}, Mn^{2+}; Roy, 1981) includes cryptomelane (K-bearing), romanèchite (Ba- and K-bearing), manjiroite (Na-bearing), coronadite (Pb-bearing), and todorokite (Ca, Na, K and Mg-bearing). Other common tetravalent manganese oxides are lithiophorite, vernadite, hollandite, and nsutite.

The manganese rocks of the Nangodi and Lawra belts contain variable amounts and textural types of manganese oxides. In manganese oxide-bearing rocks, they are the only manganese minerals present; from textural observations, they do not replace silicates. They appear as dense, massive aggregates or needle-like disseminations. Layers of oriented manganese oxides are parallel to layers of Fe hydroxide, rutile, sericite, or quartz, and some are slightly folded or crenulated. All these characteristics indicate replacement of early Mn oxide minerals. The low-reflecting, grey manganomelane minerals are relatively pure K- and Ca-bearing cryptomelane which differ from the cryptomelane of gondites by their higher Al contents and Co-Ni-dominated base metal contents (up to 0.4 wt.% CoO and 0.3 wt.% NiO; Table 5). Pyrolusite typically postdates cryptomelane formation and is commonly associated with Fe hydroxides. Its trace element contents are low. Large individual grains and aggregates of pyrolusite commonly form the central part of Mn oxide layers. In gondites, manganese oxides replace the silicate assemblage. Texturally, manganomelane minerals occur as: (1) dense, microcrystalline aggregates; (2) idiomorphic, radially-shaped needles and aggregates of needles; (3) zoned veins; and (4) as colloform, gel-like textures that replace garnet. Colour and reflectance vary considerably, suggesting the presence of different phases which are, however, intergrown on a very small (micrometer) scale. Chemically, three types can be distinguished:

(1) Manganomelane minerals in gondites significantly enriched in Ba (around 1 wt.% BaO) have between 3 and 8 wt.% BaO, and high SiO_2 (1.6–8.8 wt.%), Fe_2O_3 (2.3–10.3 wt.%), and CaO (1.6–3.4 wt.%), but low contents of Al, Mg, Na and K (Table 5). The calculated structural formulae resemble those of hollandites from the metamorphosed manganese deposits of Koduru (Sivaprakash, 1980) and Kajilidongri/India (Bhattacharya *et al.*, 1984). Hollandite is stable only in high-temperature assemblages (Neumann, 1988). Supergene Ba-bearing manganomelane minerals should be termed romanèchite rather than the former name 'psilomelane'. Spessartine rarely forms corona textures around Ba-bearing manganomelane. In one sample, layers of Ba-manganomelane are intercalated between layers of hyalophane + spessartine and spessartine + amphibole. During metamorphism, hollandite + clay may react to form hyalophane + spessartine (Bhattacharyya *et al.*, 1984). In this particular case, hollandite may be regarded as an early manganese oxide formed during metamorphism and later altered and recrystallized to form romanèchite.

(2) Manganese amphiboles, rhodonite and stilpnomelane are commonly replaced by acicular manganomelane minerals. No chemical distinction can be made with dense masses replacing garnet. These manganomelane minerals are characterized by dominance of K over Ca, by low Ba and Al contents, and by Cu values reaching 0.6 wt.% CuO (Table 5).

(3) Manganomelane minerals latest in the paragenetic sequence occur in veins crosscutting altered manganese silicates. Such veins reach 0.1–1 mm in width and are characteristically zoned: a homogeneous, grey, highly anisotropic phase in the vein core is rimmed by layers of colloform or fine-grained, inhomogeneous phases showing higher reflectance and weak anisotropism. Apparently

there are only weak chemical differences between both textural types. Manganomelane minerals in veins contain the highest K-contents measured (as much as 2.35 wt.% K_2O) and most probably are equivalent to cryptomelane (Table 5). Additionally they are characterized by low Al contents and high Cu values (as much as 0.9 wt.% CuO).

The common manganese oxide minerals known from many manganese deposits subjected to tropical weathering are rare or lacking in the samples investigated. It was not possible to prove the presence of lithiophorite and nsutite, and pyrolusite is rare compared to the manganomelane minerals. Pyrolusite and nsutite form only where weathering solutions are free of Ba or K, or where these elements are depleted by previous manganomelane development (Ostwald, 1988). If Ba and K are available, 'open tunnel structures' (such as cryptomelane and romanèchite) are preferred.

Garnet-bearing chlorite schists

Garnet-bearing chlorite schists contain isolated garnet grains as large as 0.5 mm in layers rich in chlorite (ripidolite–brunsvigite; Si = 5.1–5.9, X_{Mg} = 0.43–0.51), quartz, and albite. Accessory minerals are titanite, zircon, epidote and Fe hydroxides. Garnets show a form of sector zonation and are rimmed by manganoan calcite. They are members of the almandine–grossular–spessartine series (Fig. 3*a*; Tables 2, 3).

Geochemistry of manganese-bearing rocks

Twenty-four manganese-rich rocks from the Nangodi belt were analysed using ICP-AES (inductively coupled plasma-atomic emission spectrometry) and instrumental neutron activation (INAA) methods. The data have been published elsewhere (Melcher and Stumpfl, 1992, 1994), and only a comparison of the most relevant elements is presented here (Table 6). Manganese rocks of the Nangodi belt are chemically dominated by Si, Mn, Fe and Al; Mn/Fe values average 4.6. Multimineral gondite contains elevated Mg, Ca, and P, whereas manganese oxide-bearing phyllite is characterized by higher K and LOI values. This clearly reflects the mineralogy of the rocks: Ca- and Mg-rich rocks reacted to form garnet, amphiboles, and rhodonite, and in K-rich rocks, phengitic mica formed. K is fixed in mica as indicated by a good correlation between Al and K in phyllites. The question arises, why did manganese-bearing phyllites not react during metamorphism to form spessartine-rich garnet? Al, Mn, and Si would have been available. Assuming identical metamorphic P–T conditions for both assemblages, slight differences in bulk rock composition and in the primary mineralogy of the protolith may have been crucial for triggering the growth of garnet on one side, and of mica plus manganese oxides on the other side. In an ACF diagram (Fig. 5), whole-rock compositions of gondites plot into a field inside a triangle formed by the compositions of spessartine, Mn-actinolite, and tirodite. An Fe^{3+}/Fe^{2+} ratio of 0.1 was assumed for these rocks to calculate the plot parameters; for gondites this seems reasonable, because they do not carry any Fe^{3+}-bearing minerals (trivalent Fe in garnets and amphiboles is negligibly low). Iron in Mn-phyllites is incorporated into chlorite (probably divalent and trivalent), phengite (divalent), and Fe oxides or hydroxides (most probably primary hematite). Thus, bulk rock analyses of Mn phyllites should be calculated assuming a higher Fe^{3+}/Fe^{2+} ratio; however, changing the ratio from 0.1 to 0.5 gives only minor changes in calculated plot parameters. More drastic changes occur for some samples, when ratios > 0.5 are assumed. It has to be mentioned, that calculating Mn in its divalent state might be problematic in Mn oxide bearing-phyllites. The variable oxidation states of Mn and Fe hydroxides limit the applicability of uncorrected ACF and A′KF diagrams for these rocks.

For the bulk chemistry of rhodonite-bearing rocks (cross in Fig. 5), spessartine + Mn actinolite (Cam) + rhodonite is the stable assemblage. Samples of manganese oxide-rich phyllite plot along the join A–F outside the gondite field in or near the chlorite compositional field. The occurrence of white mica in phyllite obviously is caused by higher K contents as is indicated in the A′KF diagram. In this diagram, gondites plot along the A–F join in the chlorite and stilpnomelane fields; small amounts of stilpnomelane are observed in these rocks.

Apart from differences in major element chemistry, distinct trends in trace element contents are visible (Table 6). The manganese oxide-bearing phyllites are enriched in Nb, Pb, Rb, Sb, Sr, W, and Au relative to gondites. In addition the phyllites have totals for Cu + Co + Ni + Zn that range from 900 to 1600 ppm with Cu or Co dominating. Most gondites are Co-dominated with totals of 640–1300 ppm. Gondites are relatively enriched in Cr, Th and Zr, and may carry Ba contents up to 8000 ppm, resulting in the formation of hyalophane. Ba contents in manganese oxide-bearing phyllites range from 670 to 7600 ppm, most of which is contained in white mica.

Compared with manganese-rich rocks from other geologic environments and ages, the Nangodi manganese rocks resemble manganiferous exhalites of a submarine-hydrothermal environment. Enrichment of some trace elements (As, Cu, Ni, Zn, Ba) is typical for manganese crusts associated with submarine volcanics, and also with massive

TABLE 6. Arithmetic mean, standard deviation (s), and range of major element and selected trace element analyses of relatively unaltered manganese-rich rocks from the Nangodi belt. A — manganese oxide-bearing phyllites, B — pure gondites (ga + qz ± ilm), C — multimineral gondites (ga + qz + amp ± rdn ± hyal)

Element	A (n = 7) mean ± s	A range	B (n = 3) mean ± s	B range	C (n = 11) mean ± s	C range
SiO_2 %	45 ± 11	31–56	69 ± 6	62–73	50 ± 4	45–59
TiO_2 %	0.36 ± 0.19	0.2–0.7	0.35 ± 0.22	0.2–0.6	0.43 ± 0.13	0.2–0.6
Al_2O_3 %	7.1 ± 2.7	3.8–12.2	7.3 ± 4.0	3.6–11.5	9.4 ± 2.2	4.9–11.3
Fe_2O_3 %	7.4 ± 5.8	3.8–20.3	4.6 ± 2.5	1.8–6.7	6.2 ± 1.4	2.9–7.7
MnO %	25 ± 10	11–37	13 ± 2	11–14	22 ± 4	17–32
MgO %	0.7 ± 0.3	0.3–1.2	0.4 ± 0.2	0.2–0.6	2.0 ± 1.0	0.4–3.4
CaO %	1.2 ± 0.4	0.8–1.8	1.9 ± 0.5	1.5–2.4	4.2 ± 1.3	1.8–6.5
Na_2O %	0.37 ± 0.15	0.24–0.67	0.14 ± 0.05	0.1–0.2	0.17 ± 0.06	0.11–0.30
K_2O %	1.6 ± 0.7	0.3–2.4	0.1 ± 0.03	0.07–0.13	0.31 ± 0.22	0.11–0.81
P_2O_5 %	0.04 ± 0.04	0.01–0.1	0.05 ± 0.02	0.04–0.07	0.10 ± 0.04	0.04–0.15
LOI %	9.0 ± 2.7	6.1–12.3	2.0 ± 0.5	1.5–2.4	3.1 ± 2.5	0.7–8.5
As ppm	131 ± 127	4–370	73 ± 85	13–170	117 ± 124	9–360
Au ppb	32 ± 15	16–64	20 ± 28	3–53	11 ± 15	4–54
Ba ppm	3103 ± 2229	674–7630	24 ± 25	1–50	1840 ± 2470	94–8034
Cr ppm	49 ± 12	30–65	44 ± 7	39–52	68 ± 39	31–174
Nb ppm	81 ± 42	24–128	53 ± 34	17–84	63 ± 15	37–85
Pb ppm	50 ± 18	33–83	32 ± 12	19–43	32 ± 8	21–45
Rb ppm	30 ± 20	2–57	4.7 ± 0.6	4–5	4.4 ± 3.0	2–12
Sb ppm	18 ± 23	1–58	2.5 ± 2.5	1.8–3.1	0.6 ± 0.3	0.2–1.0
Sr ppm	502 ± 603	28–1621	53 ± 34	17–84	155 ± 130	1–376
Th ppm	1.9 ± 0.6	1.2–2.5	2.3 ± 1.7	1.1–3.5	3.7 ± 1.4	1.5–6.3
W ppm	48 ± 29	21–100	8 ± 6	4–12	12 ± 9	4–27
Zr ppm	59 ± 20	31–95	57 ± 31	32–91	94 ± 30	26–134
ΣBM ppm	1263 ± 213	987–1558	1017 ± 667	436–1746	881 ± 209	641–1295
Σ*REE* ppm	117 ± 27	86–160	78 ± 19	64–91	103 ± 32	39–146
Mn/Fe	5.4 ± 3.3	0.6–10.8	4.6 ± 3.8	1.8–8.9	4.3 ± 2.6	3.1–12.0

Data compiled from Melcher and Stumpfl (1992, 1994). LOI = loss on ignition
ΣBM = Co + Cu + Ni + Zn. Σ*REE* = sum of rare earth elements.

sulphide deposits, and the comparably high contents of such trace elements may indicate strong leaching of host rocks by hydrothermal fluids. High Co/Zn values in most samples, however, are more typical for hydrogenic deposits (Toth, 1980): Co/Zn is typically > 2.5 in hydrogenic Mn-Fe nodules, and in Nangodi manganese rocks ranges from 0.24–11. The dominance of Mn over Fe indicates strong fractionation of these metals. Chondrite-normalized rare earth element (*REE*) patterns of manganese oxide-rich phyllites reveal moderate to high enrichment of *REE* (Table 6), fractionated light *REE*s (La/Yb_{CH} = 2-17), absent to weakly negative Eu anomalies, and variably positive or negative Ce anomalies [$3Ce/(2La+Nd)_{CH}$ = 0.3–2.8], which underline the complex behaviour of Ce during precipitation and oxidation events. Gondites show a more regular, clay-like *REE* pattern and lack distinct Ce or Eu anomalies, which may be interpreted as indicating precipitation under low-temperature conditions in a relatively reducing environment, thus keeping Ce in its trivalent state. On the basis of a combination of geochemical data, Melcher and Stumpfl (1992, 1993, 1994) assume a significant hydrothermal component in the manganese rocks, which is mixed with varying proportions of volcanogenic, and very probably hydrogenic components also.

Discussion

Petrological implications and metamorphism

Mineral assemblages of the unaltered manganese-rich rocks of northern Ghana may provide information about metamorphic conditions during the Eburnean tectonothermal event. However, thermo-

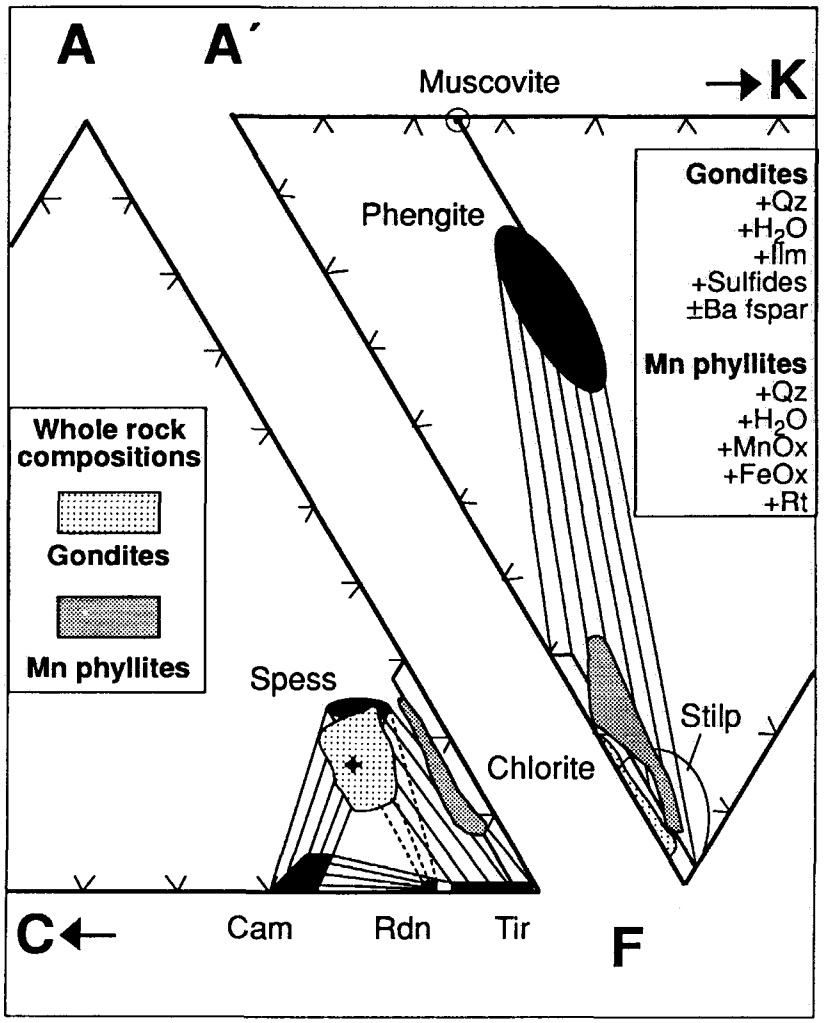

FIG. 5. Portions of ACF and A′KF diagrams. Whole-rock compositions of gondites and Mn phyllites are calculated assuming $Fe^{3+}/Fe^{2+} = 0.1$. The cross marks the whole-rock composition of a sample containing rhodonite, garnet and amphibole. Black fields outline measured compositions of spessartine garnet (Spess), calcic amphibole (Cam), rhodonite (Rdn), tirodite (Tir), stilpnomelane (Stilp), and phengite. Compositional ranges are given for chlorite (Chl) and stilpnomelane. Coexisting mineral pairs are connected by idealized tie lines. ACF and A′KF plot parameters are calculated according to Winkler (1974). Note: all Mn is calculated as MnO.

dynamic data on the Mn-rich minerals, especially in complex multicomponent systems, are almost lacking. Disequilibrium textures are commonly observed and provide an additional constraint on the use of thermodynamic models. Therefore, stability ranges of minerals observed in Ghanaian gondites are discussed by comparison with published data from natural occurrences elsewhere.

Four different mineral assemblages are observed in manganese rocks of northern Ghana:

(1) Mn-oxide + Fe-oxide + rutile + sericite + chlorite + quartz (Mn oxide-bearing phyllites);
(2) Chlorite + quartz + albite + garnet + epidote (garnet-bearing chlorite schists);
(3) Garnet + quartz ± ilmenite/rutile (pure gondites);
(4) Garnet + quartz + rhodonite + hyalophane + calcic amphibole + tirodite/dannemorite + stilpnomelane/manganophyllite + ilmenite/rutile (multimineral gondites).

Assemblages (2) to (4) contain garnet of

TABLE 7. Chemical, mineralogical and metamorphic parameters of tirodite- and dannemorite-bearing assemblages. Variations in X_{Mg} [Mg/(Mg+Fe)] and X_{Mn} [Mn/(Mn+Mg+Fe)] of amphiboles, associated Mn-bearing minerals, and estimated T–P conditions of metamorphism

	Locality	X_{Mg}Amp	X_{Mn}Amp	Mn-mineral assemblage	T(°C)	P(kbar)	Ref.
(1) *Tirodite-bearing assemblages*							
AM	Aar Massif	0.85	0.21	Cam	350–400	1–3	A
BK	Bald Knob			Sp+Rdc+Rdn+Pxm+Tph+So+Ilm	>550	5	F
BT	Balmat, Talcville	0.99	0.19		625±25		S
BU	Buritirama	0.94	0.33–0.35	Sp+Cam+Rdc+Mph+Pxm+Tph	500–550	3	P1
CH	Chikla	1.0	0.15	Sp+Rdn+Brn	600±20	6	R1
ML	Mattagami Lake	0.52–0.61	0.19–0.21	Pym+Cam+Bio+Chl	440	3	P2
NB	Nangodi Belt	0.58–0.77	0.20–0.34	Sp+Cam+Rdn+Stilp/Mph+Qz	450–500	2–3	M
NIG	Nigeria	0.50–0.75	0.11–0.21	Sp+Cam+Rdc+Ilm	540–610		N
	Nsuta	0.97	0.36	Sp+Rdn	500?		J1
	Sambagawa	0.95	0.25				H
SA	Sausar Fm.	0.95–0.99	0.30–0.36	Sp+Pxm±Rdc	650	6	D
TI	Tirodi	1.0	0.12	Sp+Rdn	650±25	6	
WA	Wabush IF	0.73–0.88	0.24–0.30	Qz+Cum+Hm; Rdn+Cald+Rdc	<600	6–10	K1,2
2) *Dannemorite-bearing assemblages*							
	Dongfenshan	0.17	0.11	Gru+Cam			L
GB	Gamsberg	0.14	0.10	Sp+Ol+Opx+Pxm/Rdn+Cam	630–670	3–5.5	R2
GR	Grythyttan	0.33	0.22	Sp+Rdc+Stilp+Pxm(±Rdn)+Chl	400–425		O
LB	Lawra Belt	0.38	0.24–0.26	Sp+Mph+Qz	>500?		M
NIG	Nigeria	0.13–0.36	0.11–0.29	Sp+Cam+Rdc+Pxm+Opx+Tph+Ilm	610		N
PN	Papua New. G.	0.45	0.29	De+Stilp	200–300	4–6	W
	Poland	0.03–0.06	0.08–0.12		300–440		J2

Minerals: Bio — biotite, Brn — braunite, Cald — calderite , Cam — calcic amphibole, Chl — chlorite, Cum — cummingtonite, De — deerite, Gru — grunerite, Hm — hematite, Ilm — ilmenite — pyrophanite, Mph — manganophyllite, Ol — olivine, Opx — orthopyroxene, Pxm — pyroxmangite, Pym — pyrosmalite, Qz — quartz, Rdc — rhodochrosite, Rdn — rhodonite, So — sonolite, Sp — spessartine, Stilp — stilpnomelane,Tph — tephroite. References: A — Abrecht (1989), D — Dasgupta *et al.* (1988), F — Flohr (1992), H — Hashimoto (1990), J1 — Jaffe *et al.* (1961), J2 — Janeczek (1989), K1 — Klein (1964), K2 — Klein (1966), L — Liu (1987), M — Melcher (this work), N — Neumann (1988), O — Oen *et al.* (1986), P1 — Peters *et al.* (1977), P2 — Pan and Fleet, (1993), R1 — Roy (1974), R2 — Rozendaal and Stumpfl (1984), S — Segeler (1961), W — Worthing (1987).

characteristic compositions (Fig. 3*a*). Garnet in assemblage (2) is relatively poor in Mn and enriched in Fe and Ca. In assemblage (3) it is either very Mn-rich (spessartine 80–87), when hosted by metavolcanics, or slightly enriched in Fe (spess 70–84), when hosted by metasedimentary rocks. Garnet in assemblage (4) spans a range from spess 60–85. Thus, bulk rock composition controls garnet composition; and as it has been discussed above, bulk rock composition is closely related to primary depositional features, making garnet composition a valuable tool in deducing, for example, the distance from source areas of hydrothermal solutions (Melcher and Stumpfl, 1994).

Spessartine-rich garnet is stable across the range of metamorphic conditions, beginning with the low greenschist facies (400°C, 2 kbar; Hsu, 1968). The absence of almandine garnet in more pelitic, Mn-poor pyroclastic and sedimentary rocks of the Nangodi belt points to metamorphic conditions below the almandine isograd in metapelitic rocks (Winkler, 1974). Spessartine-rich garnet with ilmenite inclusions is observed in some gondites and typically would make a good geological thermometer (Pownceby *et al.*, 1987). However, the ilmenite is altered to pseudorutile and partly exchanged with matrix minerals (quartz). As a result, the garnet–ilmenite geothermometer gives unrealistically low metamorphic temperatures of < 250°C. During (pre-metamorphic) ilmenite alteration, MnO was mobilized and no equilibrium was attained for garnet–pseudorutile pairs.

Manganese amphiboles are observed in amphibolite facies assemblages worldwide. Some occurrences of

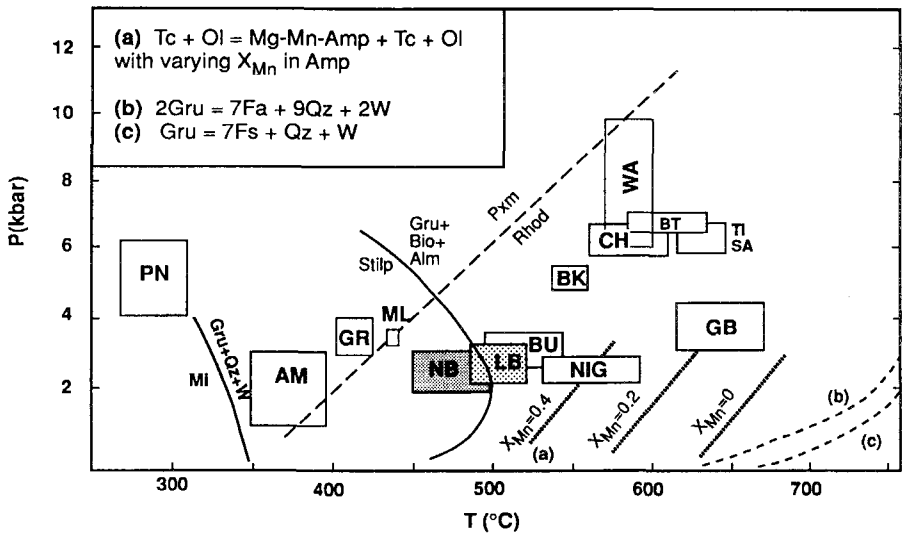

FIG. 6. Evaluation of metamorphic pressure-temperature conditions for gondites in the Nangodi (NB) and Lawra belts (LB), northern Ghana, based on comparison with literature data. Boxes indicate $P-T$ ranges of manganese amphibole-bearing assemblages (abbreviations explained in Table 7). The following reaction lines are projected: Pyroxmangite → Rhodonite (Maresch and Mottana, 1976); a stilpnomelane-consuming reaction according to Miyano and Klein (1989); Mg-Mn amphibole-creating reactions (a) inferred from Maresch and Czank (1988). The grunerite-consuming reactions (b) and (c), and the reaction Mi → Gru + Qz + W are taken from Klein (1983). Additional abbreviations not used in Table 7: Alm — almandine, Fa — fayalite, Fs — ferrosilite, Mi — minnesotaite, Pxm — pyroxmangite, W — water.

tirodite and dannemorite, their chemical characteristics and mineral assemblages, are summarized in Table 7. In Fig. 6, $P-T$ boxes for these occurrences are given, if temperature and pressure conditions are known from independent geological thermo- and barometers. In the system $MgSiO_3$–$MnSiO_3$–SiO_2–H_2O, manganoan cummingtonite forms by reaction of olivine and talc at low temperature, and of orthopyroxene, quartz, and water at high temperature (Huebner, 1986). Experimentally deduced temperatures depend on the Mn/(Mn+Mg) value of the minerals. Temperature estimates range from 400 to 620°C for the lower, and from 570 to 750°C at 2 kbar for the upper stability limit of manganoan cummingtonite at Mn/(Mn+Mg) decreasing from 0.3 to 0. Maresch and Czank (1988) synthesized Mn–Mg amphiboles at 625–775°C and 1–6 kbar from gels and observed complicated structural disordering. Extrapolation of the three-phase loop (amphibole + talc + olivine) proposed by these authors towards lower temperatures yields a lower temperature stability limit near 510°C for Mn–Mg amphibole of the composition Mn/(Mn+Mg) = 0.4 and Mg/(Mg+Fe) = 1 coexisting with talc and olivine (2 kbar). Tirodite analyses from the Nangodi belt average to Mn/(Mn+Mg) = 0.4, and Mg/(Mg+Fe) ranges between 0.58 and 0.77. Incorporation of Fe should result in a slight decrease of the stability limit. Dasgupta *et al.* (1988) made petrological observations of natural manganese amphibole-bearing assemblages in the amphibolite facies metamorphic grade. In all cases examined, Mg–Mn amphibole was associated with carbonate and pyroxene ± rhodonite/pyroxmangite. Tirodite was interpreted to form from carbonate-silica precursors during decarbonation under unbuffered X_{CO_2} (Dasgupta *et al.*, 1988, 1990).

Calcic amphibole coexisting with tirodite is rarely reported in the literature. Figure 4 shows a pronounced miscibility in Ca between the calcic amphiboles and tirodite. Although some authors (Klein, 1964) have suggested, that the addition of Mn diminishes the miscibility gap between coexisting monoclinic cummingtonite and calcic amphibole, the high Ca contents in Nangodi tirodites are surprising. Calcic amphiboles carry higher Mg, Ca, and Al than coexisting tirodites which are enriched in Mn and Fe. The tie lines between calcic amphiboles and tirodites show a negative slope and are parallel to tie lines constructed for samples from Buritirama, Brazil (500–550°C; Peters *et al.*, 1977).

In summary, the compositions of naturally occurring manganese amphiboles are of restricted use in deducing metamorphic conditions, because in most cases they are not 'simple' binary solid solutions. Amphibole composition strongly depends on bulk rock chemistry, as shown by the occurrence of dannemorite over a wide $P-T$ range in Fe-rich rocks (Fig. 6). The available data show that at higher metamorphic grades (upper amphibolite facies) most Mn–Mg–Fe-bearing rocks host pure Mg–Mn cummingtonite, although in low-grade rocks, Fe substitutes for Mg in considerable amounts. Manganese amphiboles in high-pressure and contact-metamorphic parageneses typically contain elevated alkali contents.

Manganese-bearing pyroxene, which would clearly indicate amphibolite facies conditions, is not present in northern Ghanaian gondites. The absence of pyroxmangite, which is stable at relatively higher pressures than rhodonite (Maresch and Mottana, 1976), indicates a temperature higher than the pyroxmangite–rhodonite transition (475–500°C at an estimated regional metamorphic pressure of 2–4 kbar; Dasgupta and Manickavasagam, 1981). However, the presence of Ca, Fe and Mg in rhodonite also has to be taken into account.

In metamorphosed banded iron formations, stilpnomelane reacts to form grunerite, almandine and biotite at 430–470°C and maximum pressures of 5–6 kbar (Miyano and Klein, 1989). In the Mn system, an analogous reaction of Mn-stilpnomelane to tirodite + spessartine + manganophyllite may be postulated. There is no information about a shift, or the direction of a shift of the reaction curve with incorporation of manganese in stilpnomelane.

The composition of Ba-bearing K-feldspar may provide temperature estimates because there are several zones of immiscibility along the Ba-K join. For Na-poor compositions on the Ba-poor limb of the lowest-celsian solvus, McSwiggen *et al.* (1994) assume equilibration temperatures for natural assemblages. Hyalophane from Nangodi gondites contains between 17 and 32 mol.% celsian. A metamorphic temperature around 500°C would result, if the composition of an exsolved Ba-feldspar in the Cuyuna Range (celsian 9 and 19 mol.%; McSwiggen *et al.*, 1994) is taken into account, and the lowest Ba composition in the assemblage reported here (celsian 17 mol.%) is on the Ba-rich limb of the lowest-celsian solvus. Furthermore, the presence of hyalophane points to a hydrothermal system introducing Ba. Ba-rich rocks in the Nangodi belt may also give hints to as yet undiscovered massive sulphide concentrations in the area (Melcher and Stumpfl, 1993, 1994).

In the $P-T$ diagram (Fig. 6), the Fe-stilpnomelane reaction curve of Miyano and Klein (1989) and the rhodonite/pyroxmangite transition of Maresch and Mottana (1976) are added to $P-T$ boxes representing natural manganese amphibole-bearing assemblages. Metamorphic conditions for gondites of the Nangodi belt are assumed to be close to the boundary between upper greenschist and lower amphibolite facies. Many parameters point to disequilibrium conditions in Nangodi gondites, e.g. reactions between calcic amphibole and tirodite, mantling of amphibole domains with garnet (Fig. 2*c*), and the occurrence of both Mn-stilpnomelane and manganophyllite. Staurolite and garnet are described in schists surrounding manganese rocks in the Lawra belt (Roudakov, 1965), indicating amphibolite grade metamorphism. In manganese rocks of the Lawra belt, stilpnomelane and manganoan actinolite are lacking, and dannemorite is stable.

Precursor sediments

In order to work out a model for the depositional environment of metamorphosed manganese rocks, primary mineral phases must first be established. Possible primary minerals may be deduced from a process of simple elimination. Protoliths of gondites could be (1) very fine-grained manganese oxide–clay mixtures, (2) Mn carbonates (e.g. Dasgupta *et al.*, 1990, 1992), or (3) primary Mn silicate gels (Huebner *et al.*, 1992). Dasgupta *et al.* (1990) admit that the precursor of Mn-silicate rocks with minor oxides is problematic, but favour higher oxides or hydroxides of Mn and Fe admixed with clay and quartz; as mentioned earlier, assemblages containing Mn amphiboles are interpreted as having developed through decarbonation reactions from carbonate precursor sediments (Dasgupta *et al.*, 1988). Manganese-silicate rocks in greenstone belts of northern Ghana do not include primary Mn^{4+} or Mn^{3+} oxides (e.g. hausmannite) or silicates (e.g. braunite), or Mn^{2+} carbonates. Such minerals may have been completely destroyed during deoxidation and metamorphism to form Mn^{2+} silicates. However, the association of manganese silicates with premetamorphic ilmenite and sulphides, and the absence of hematite in most gondite samples of the Nangodi belt suggest reducing conditions during manganese precipitation. The f_{O_2}/f_{S_2} conditions may have been unfavourable to the formation of higher Mn^{3+} or Mn^{4+} oxides, and probably were similar to those calculated for the Bald Knob deposit in North Carolina (Winter *et al.*, 1981). Thus, possibilities (2) or (3) may be favoured. Furthermore, there are no relics of carbonates preserved in the Nangodi gondites. Manganese rocks of slightly higher metamorphic grade and similar major element chemistry in Nigeria have preserved carbonate relics as inclusions in Mn garnets (Neumann,

1988). Manganese carbonates are present in many manganese protores of southern Ghana (Kesse, 1976), and also form a considerable part of the protore at the Nsuta deposit (e.g. Kleinschrot *et al.*, 1993). There are two possibilities left: manganese protoliths were originally free of carbonates, or carbonates have been completely dissolved or reacted to form, for example, manganoan calcic amphibole and tirodite. Petrographic observations in adjacent rocks show that carbonates are still present, e.g. as carbonate-bearing sedimentary rocks, and as hydrothermal alteration products in metavolcanics. Carbonates in carbonate-bearing rocks of Ghana have been interpreted to be pre-tectonic and not connected with alteration and metamorphic processes (Hirdes and Leube, 1989; Leube *et al.*, 1990). In the Nangodi belt, carbonate-bearing rocks occur principally in the same transition zone as manganese rocks, and it seems unlikely, that carbonates have been completely removed from the Mn sediments, and preserved in the adjacent Mn-free sediments.

For submarine lens-shaped Mn accumulations in the Franciscan Complex of California, Huebner *et al.* (1992) conclude that Mn^{2+} may be leached from volcanic rocks or sediments by mildly reducing and acidic fluids, transported to the seafloor and precipitated either as Mn^{2+} and Mn^{3+} oxides, silicates, or carbonates. Manganese silicate gels would form if enough soluble silica is present. In the Nangodi belt, soluble silica may have been present as volcanic glass; the intensive interlayering with hydrothermal chert also indicates the availability of silica-rich solutions. Mn carbonates would form, if (organic or juvenile) carbon is present, and organic debris at the seafloor would furthermore prevent Mn^{2+} from oxidation by seawater and precipitation as Mn^{4+}-oxides or oxyhydroxides. If soluble silica or carbon is absent, only quadrilateral Mn oxides may form as recently found at submarine manganese deposits along oceanic ridges. The amount of Al necessary to form Mn-rich garnet is explained by the formation of primary Al-bearing clays from either weathering of volcanic rocks or periodic input of air-fall pyroclastic material. During metamorphism, Mn-rich silica gels (containing sulphides) reacted with Al–Mg–Fe-rich clays to form the gondite assemblage.

Dasgupta *et al.* (1992) showed that Mn-oxide rocks and Mn-silicate rocks with minor Mn oxides (gondites) of the Early Proterozoic Sausar Group, India, evolved from primary Mn oxides through deoxidation equilibria during prograde metamorphism. The sediments were deposited on an oxidized substrate in shallow marine basin margins without any significant volcanic or hydrothermal component. Metals are derived from upwelling of anoxic deep seawater (Force and Cannon, 1988) and precipitated above the anoxic–oxic boundary. In the Late Proterozoic Penganga Group of India, primary manganese oxide minerals are preserved in sedimentary manganese-oxide ores interstratified with chert and calcareous shale (Roy *et al.*, 1990). Primary sedimentary todorokite and birnessite are converted to manganite, braunite and bixbyite during late diagenesis, implying reduction of quadrivalent to tri-and divalent Mn minerals. Pyrolusite and cryptomelane occur as supergene alteration products.

Textural and chemical evidence suggests that manganese oxide-bearing phyllites of northern Ghana may have been deposited in shallow marine basins as primary Mn oxides or hydroxides interlaminated with quartz, Fe oxides or hydroxides, and tuffaceous materials. Cryptomelane and pyrolusite, the prevailing manganese minerals, most probably are supergene alteration products of earlier oxides or hydroxides. Cryptomelane, some of which preserves a laminated microcrystalline fabric with goethite, rutile and chert, may replace minerals such as todorokite or birnessite.

Because no primary manganese minerals are preserved either in gondites or in manganese phyllites, evaluation of a precursor mineralogy is highly speculative. Nevertheless, these manganese rocks were apparently deposited in two different geochemical environments and do not represent different diagenetic or metamorphic conditions. Manganese phyllites were deposited on an oxidized substrate as oxides, probably underwent diagenetic and metamorphic deoxidation to Mn^{3+} or Mn^{2+} oxides, and were recently oxidized in a tropical climate to supergene Mn^{4+} minerals. Manganese silicate rocks were deposited in a slightly reducing environment (in the stability fields of pyrrhotite and manganoan ilmenite) as Mn-silicate gels or probably as carbonates, and underwent early oxidation (documented by the pre-metamorphic formation of pseudorutile from primary manganoan ilmenite), and subsequent oxidation, dehydration, and decarbonation reactions (probably in the case of amphibole-bearing assemblages) to form Mn^{2+}-Fe^{2+} silicates. Manganese silicates are more resistant to supergene alteration, and therefore only small amounts of secondary manganomelane and pyrolusite are encountered in massive gondites.

Geological environment

Manganese-bearing rocks in Early Proterozoic greenstone belts of northern Ghana are associated with chert, volcaniclastic rocks and tholeiitic MOR-type basalt. A relatively complete ophiolitic sequence 1.5–2 km thick in the northern Bole-Navrongo belt has been mapped by Carlson (1992). Besides the now well-established nature of the Nangodi greenstones

as oceanic MOR-basalts (Sylvester and Attoh, 1992; Melcher and Stumpfl, 1992, 1994; Melcher, 1993), komatiitic lava flows, a sheeted dyke interval, massive pyroxene gabbro, and some serpentinized ultramafic rocks were also found. The tholeiitic basalts are spatially associated with calc-alkalic rocks in northern Ghana, but these are considered as being younger because apophyses of comagmatic calc-alkalic granitoids in places intrude the manganese-bearing rocks. Associated argillitic strata typically carry lithic volcanic clasts. Soft-sediment deformation is very common in the chemical sediments. Rocks pointing to continental erosion (e.g. quartz detritus) are absent. In view of all these facts, northern Ghanaian manganese-bearing rocks are similar to ophiolite-hosted manganese deposits associated with oceanic spreading centres (e.g. Apennin; Bonatti *et al.*, 1976). In the classification of volcanogenic manganese deposits developed by the US Geological Survey, they most closely resemble the Cyprus type (Mosier and Page, 1988): this type is developed as lenticular bodies of umber (manganiferous Fe-rich sedimentary rocks) overlying pillow-basalt flows at the base of a sedimentary sequence, and is either attributed to deep or shallow marine deposition in an interarc-basin, or in a mid-oceanic ridge setting. Volcanogenic manganese deposits — Franciscan, Cuban, Olympic Peninsula, and Cyprus type (Mosier and Page, 1988) — are enriched in Mn, Fe, Cu and Ba, and Cyprus-type sediments are additionally enriched in Co, Ni and Zn. The major difficulties in attributing the Nangodi manganese rocks to the Cyprus-type are the significantly higher Mn/Fe ratios in Nangodi and the oxide- and silicate-dominated mineralogy; Cyprus umbers consist of amorphous manganese hydroxides, goethite, and maghemite, and no discrete manganese mineral has been found in them to date (Robertson and Hudson, 1973). The higher Mn/Fe ratio in Nangodi may be explained by considerably higher fractionation of Fe from Mn in the hydrothermal fluids. The problems concerning the precursor minerals have been discussed in a previous section. It is most likely that the Nangodi manganese rocks represent metamorphosed, modified (e.g. Mn-rich) Cyprus-type volcanogenic manganese accumulations in peripheral parts of a spreading centre. This implies the probability of massive sulphide deposits in the stratigraphic sequence.

Conclusion

Chemical sediments in northern Ghanaian greenstone belts were deposited in an oceanic environment, relatively close to a mid-oceanic ridge or spreading centre, along fracture zones providing the seawater with relatively hot (> 300°C?), acid and reducing hydrothermal solutions. These may represent either late-stage juvenile-volcanic emanations or, more likely, ascending waters of a deep, heat-driven seawater convection system penetrating large amounts of volcanic rocks. Elements like Fe, Mn, Ba, Si and trace metals (Cu, Ni, Zn, Au) are readily leached from basalt and vented onto the seafloor. Introduction of SO_4^{2-} by seawater may help to separate Fe from Mn. Iron and S will readily precipitate as sulphides whereas Mn will reach the sediment-water interface and precipitate as an oxide, silicate or carbonate.

In places, tholeiitic volcanic rocks in the Nangodi belt reveal strong hydrothermal alteration (pre-metamorphic autohydrothermal chlorite-muscovite alteration; Leube *et al.*, 1990), accompanied by disseminations of Fe–Ni–Cu sulphides. The presence of tourmalinites in the uppermost parts of the volcanic sequence is strong evidence for circulation of hydrothermal fluids along the belt-basin boundaries (Melcher and Stumpfl, 1994). Tourmalinites form along fluid pathways where boron-rich hydrothermal solutions enter host rocks of suitable composition. Tourmaline and quartz replace magmatic minerals within a porphyritic volcanic rock. Such replacement of permeable host rocks in upper parts of submarine-hydrothermal systems, as described by Slack *et al.* (1993), has been demonstrated for the Birimian syngenetic Yaouré-Angovia gold deposit, Ivory Coast (Milési *et al.*, 1989).

The enrichment of Mn over Fe in all manganese deposits of the Eburnean province suggests a very powerful separation mechanism. To date no true Fe-rich equivalents to the banded manganese rocks were described in the Birimian of Ghana. Iron-formations, which are so overwhelmingly important in Early Proterozoic successions of, for example, the Superior Province, have not been observed in the Birimian Supergroup of West Africa. In the Nangodi belt, a thin layer of ferruginous oolitic chert crops out in a sequence of coarse volcaniclastic rocks overlying basalts (Melcher and Stumpfl, 1992, 1994). These rocks carry mm-sized ovaloid globules of Fe oxyhydroxides in a cherty and volcaniclastic matrix. They probably were deposited in shallow water; a low Co/Zn value (< 0.02) points to a hydrothermal influence.

The absence of large amounts of Fe-rich chemically precipitated strata indicates that most of the iron must have been either precipitated before the manganese, or transported away and diluted by other material. Volcanic flows in places are enriched in pyrrhotite and chalcopyrite, and Fe-sulphide-bearing sedimentary rocks occur in the transition zone as parts of the chemical facies. Although most of the abundant pyrite present today is clearly of post-

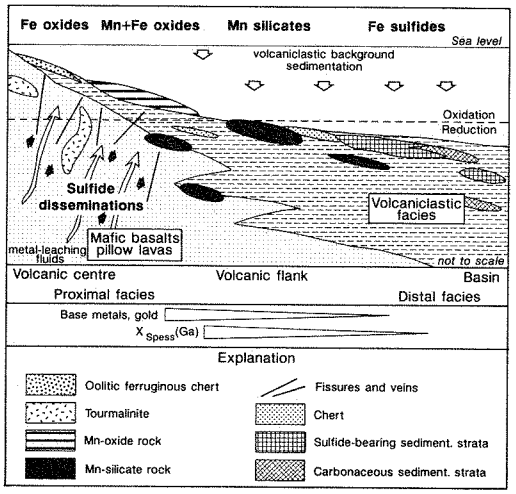

FIG. 7. Schematic model of facies relationships between chemical sediments, volcanic and volcaniclastic rocks in Birimian greenstone belts of northern Ghana.

depositional, most likely metamorphogenic origin, such mixed pyroclastic and chemical sediments may have been the traps where part of the Fe was originally precipitated.

Accordingly, Mn was precipitated in at least two distinctly different environments: in a relatively oxidized environment later forming manganese oxide-bearing phyllite, and in a more reducing environment in the presence of soluble silica forming gondite during metamorphism. Base metal and gold contents are higher in the first group, pointing to a more proximal deposition with respect to a hydrothermal source. The presence of both types of manganese rocks in one belt, but only rarely in an intimate interlayering, suggests some kind of a facies zonation within the chemical deposits. Leube and Hirdes (1990) developed a facies concept to explain the contemporaneous deposition of volcanic rocks in volcanic belts, and deposition of volcaniclastic rocks in metasedimentary-volcaniclastic basins of the Birimian Supergroup in Ghana. From the volcanic belt towards the basin centre, the facies types are as follows: volcanic-volcaniclastic facies → wacke (turbidite) facies → volcaniclastic-argillite facies → argillite facies. In addition, a chemical facies is present in the volcanic-volcaniclastic facies, and in transition zones between belts and basins, and also extends into the basins.

It is assumed that volcanic edifices in a mid-oceanic rifting environment reached sea-level (Fig. 7) and provided enough heat to generate a seawater convection sytem. On the flanks of the volcanoes, chemical sediments precipitated. In shallower water, oolitic ferruginous chert formed under the influence of proximal hydrothermal solutions (Fe-dominated, very low Co/Zn), followed by clays rich in base metals, manganese and iron. In deeper parts of the basin, below an anoxic–oxic boundary, manganese silicate gels and chert precipitated from cooled solutions slightly depleted in metals and with higher Mn/Fe values. Manganese may have been transported over considerable distances and precipitated in distal positions as silicates under high admixture of volcanigenic detritus: garnet-bearing chlorite schist formed from these rocks during subsequent regional metamorphism. The assumed stratification in the relatively shallow waterbody to produce the necessary oxidation boundary may have existed only in periods of volcanic and tectonic quiescence, and remote from the shelf edge and its turbidity currents.

Acknowledgements

This study formed part of a Ph.D. thesis carried out at the Mining University, Leoben, and is based on field and analytical work conducted within the context of the 'Chemical facies and gold mineralization in northern Ghana' project (financed by the German Federal Institute for Geosciences and Natural Resources, Hannover). Special thanks are due to E.F. Stumpfl (Leoben) who guided me through the project from the very beginning. The late Alfred Leube (München), formerly Professor at the German Federal Institute for Geosciences and Natural Resources (Hannover), initiated the project, introduced me to the geology of Ghana, and was an indefatigable source of ideas and information throughout the work. I therefore dedicate this publication to his memory. I gratefully acknowledge the help and support of Director G.O. Kesse and his staff of the Ghana Geological Survey, and the members of the Institute of Geological Sciences (Leoben). The ICP-AES whole-rock analyses were carried out by R. Tessadri (Innsbruck). H. Muehlhans (Leoben), and E. Mersdorf (Innsbruck) kindly provided help with microprobe analysis. Critical reviews by G.B. Morey, P.L. McSwiggen, N. Balaban (St. Paul), and by an anonymous reviewer of Mineralogical Magazine, are gratefully acknowledged. This paper was completed during the tenure of a postdoctoral fellowship at the Minnesota Geological Survey (St. Paul) provided by the German Academic Exchange Service (DAAD).

References

Abouchami, W., Boher, M., Michard, A. and Albarede, F. (1990) A major 2.1 Ga event of mafic magmatism

in West Africa: an early stage of crustal accretion. *J. Geophys. Res.*, **95**, 17605–29.

Abrecht, J. (1989) A hydrothermal manganiferous sulfide assemblage in Carboniferous volcanic rocks of the central Aar massif (Switzerland). *Schweiz. mineral. petrogr. Mitt.*, **69**, 117–128.

Attoh, K. (1982) Structure, gravity models and stratigraphy of an early Proterozoic volcanic-sedimentray belt in northeastern Ghana. *Precamb. Res.*, **18**, 275–90.

Bence, A.E. and Albee, A.L. (1968) Empirical correction factors for the electron microanalysis of silicates and oxides. *J. Geol.*, **76**, 382–403.

Bhattacharyya, P.K., Dasgupta, S., Fukuoka, M. and Roy, S. (1984) Geochemistry of braunite and associated phases in metamorphosed non-calcareous manganese ores in India. *Contrib. Mineral. Petrol.*, **87**, 65–71.

Bjerg, S.C., Mogessie, A. and Bjerg, E. (1992) HYPERFORM — a Hypercard program for Macintosh microcomputers to calculate mineral formulae from electron microprobe and wet chemical analysis. *Computers & Geosci.*, **18**, 717–45.

Bilgrami, S.A. (1956) Manganese silicate minerals from Chikla, Bhandara district, India. *Mineral. Mag.*, **31**, 236–44.

Bonatti, E., Zerbi, M., Kay, R. and Rydell, H. (1976) Metalliferous deposits from the Apennine ophiolites: Mesozoic equivalents of modern deposits from oceanic spreading centers. *Geol. Soc. Amer. Bull.*, **87**, 83–94.

Carlson, Ch. (1992) Recognition of a Birimian ophiolite allochthon in the Nangodi Greenstone Belt, N.E. Ghana. *Geol. Soc. Africa, 9th Int. Geol. Conf., Regional Trends in African Geology, Nov. 1992, Program and Abstracts*, 10–11, Accra, Ghana.

Choubert, B. (1973) Occurrences of manganese in the Guianas (South America) and their relation with fundamental structures. *UNESCO, Earth Sci. Ser.*, **9**, 115–24.

Dasgupta, H.C. and Manickavasagam, R.M. (1981) Regional metamorphism of non-calcareous manganiferous sediments from India and the related petrogenetic grid for a part of the system Mn–Fe–Si–O. *J. Petrol.*, **22**, 363–96.

Dasgupta, S., Banerjee, H., Fukuoka, M., Bhattacharya, P.K. and Roy, S. (1990) Petrogenesis of metamorphosed manganese deposits and the nature of the precursor sediments. *Ore Geol. Rev.*, **5**, 359–84.

Dasgupta, S., Bhattacharya, P.K., Chattopadhyay, G., Banerjee, H., Majumdar, N., Fukuoka, M. and Roy, S. (1988) Petrology of Mg–Mn amphibole-bearing assemblages in manganese silicate rocks of the Sausar Group, India. *Mineral. Mag.*, **52**, 105–11.

Dasgupta, S., Fukuoka, M. and Roy, S. (1984) Hematite–pyrophanite intergrowth in gondite, Chikla area, Sausar Group, India. *Mineral. Mag.*, **48**, 558–60.

Dasgupta, S., Roy, S. and Fukuoka, M. (1992) Depositional models for manganese oxide and carbonate deposits of the Precambrian Sausar Group, India. *Econ. Geol.*, **87**, 1412–8.

Eggleton, R.A. and Chappell, B.W. (1978) The crystal structure of stilpnomelane. Part III: Chemistry and physical properties. *Mineral. Mag.*, **42**, 361–8.

Flohr, M.J.K. (1992) Geochemistry and origin of the Bald Knob manganese deposit, North Carolina. *Econ. Geol.*, **87**, 2023–40.

Force, E.R. and Cannon, W.F. (1988) Depositional model for shallow-marine manganese deposits around black shale basins. *Econ. Geol.*, **83**, 93–117.

Frost, M.T., Grey, I.E., Harrowfield, I.R. and Mason, K. (1983) The dependence of alumina and silica contents on the extent of alteration of weathered ilmenites from Western Australia. *Mineral. Mag.*, **47**, 201–8.

Gardiner, W.W. and Venugopal, D.V. (1992) Spessartine-quartz rock (coticule) occurrences in New Brunsvick, Canada, and their use in exploration for massive sulphide, tin–tungsten and gold deposits. *Trans. Instn. Mining Metall. (Sect. B: Appl. Earth Sci.)*, **101**, 147–57.

Ghose, S. and Hexiong, Y. (1989) Mn–Mg distribution on a *C*2/m manganoan cummingtonite: crystal-chemical considerations. *Amer. Mineral.*, **74**, 1091–6.

Goodwin, A.M. (1991) *Precambrian Geology. The dynamic evolution of the continental crust.* Academic Press, London, 666 pp.

Hashimoto, M., Funakoshi, R. and Kusakabe, K. (1990) Manganese-rich amphibole from quartz schists of the Iimori district, Sambagawa terrane, Wakayama. *Ganko*, **85**, 481–7.

Hirdes, W. and Leube, A. (1989) On gold mineralization of the Proterozoic Birimian Supergroup in Ghana/West Africa. *Unpubl. report*, 179 pp., Bundesanstalt für Geowissenschaften und Rohstoffe, Hannover (BGR Archive No. 104248).

Hirdes, W., Davis, D.W. and Eisenlohr, B.N. (1992) Reassessment of Proterozoic granitoid ages in Ghana on the basis of U/Pb zircon and monazite dating. *Precamb. Res.*, **56**, 89–96.

Hsu, L.C. (1968) Selected phase relationships in the system Al–Mn–Fe–Si–O–H: A model for garnet equilibria. *J. Petrol.*, **9**, 40–63.

Huebner, J.S. (1986) Nature of phases synthesized along the join $(Mg,Mn)_2Si_2O_6$. *Amer. Mineral.*, **71**, 111–22.

Huebner, J.S., Flohr, M.J.K. and Grossman, J.N. (1992) Chemical fluxes and origin of a manganese carbonate-oxide-silicate deposit in bedded chert. *Chem. Geol.*, **100**, 93–118.

Jaffe, H.W., Meyer, W.O.J.G. and Selchow, D.H. (1961) Manganoan cummingtonite from Nsuta, Ghana. *Amer. Mineral.*, **46**, 642–53.

Jakob, J. (1933) Die Manganerzlagerstätten zwischen Val d'Err und Roffna (Oberhalbstein), ihre Begleitminerale und ihre Genesis. *Schweiz. mineral. petrogr. Mitt.*, **13**, 17–39.

Janeczek, J. (1989) Manganoan fayalite and products of its alteration from the Strzegom pegmatites, Poland. *Mineral. Mag.*, **53**, 315–25.

Kesse, G.O. (1976) The Manganese Ore Deposits of Ghana. *Ghana Geol. Survey Bull.*, **44**.

Kesse, G.O. (1985) *The mineral and rock resources of Ghana*. A.A. Balkema, Rotterdam & Boston, 610 pp.

Klein, C. (1964) Cummingtonite–grunerite series: a chemical, optical and X-ray study. *Amer. Mineral.*, **49**, 963–82.

Klein, C. (1966) Mineralogy and petrology of the metamorphosed Wabush Iron Formation, southwestern Labrador. *J. Petrol.*, **7**, 240–305.

Klein, C. (1983) Diagenesis and metamorphism of Precambrian banded iron-formations. In *Iron-Formation: Facts and Problems* (Trendall, A.F. and Morris, R.C. eds.). Elsevier, 417–69.

Kleinschrot, D., Klemd, R., Bröcker, M., Okrusch, M., Franz, L. and Schmidt, K. (1993) The Nsuta Manganese Deposit, Ghana: Geological Setting, Ore-forming Process and Metamorphic Evolution. *Z. Angew. Geol.*, **39**, 48–50.

Kramm, U. (1976) The coticule rocks (spessartine quartzites) of the Venn-Stavelot Massif, Ardennes, a volcanoclastic metasediment? *Contrib. Mineral. Petrol.*, **56**, 135–55.

Krosse, S. and Schreyer, W. (1993) Comparative geochemistry of coticules (spessartine-quartzites) and their red schist country rocks in the Ordovician of the Ardennes Mountains, Belgium. *Chem. Erde*, **53**, 1–20.

Leake, B.E. (1978) Nomenclature of amphiboles. *Mineral. Mag.*, **42**, 533–63.

Leube, A., Hirdes, W., Mauer, R. and Kesse, G.O. (1990) The early Proterozoic Birimian Supergroup of Ghana and some aspects of its associated gold mineralization. *Precamb. Res.*, **46**, 139–65.

Liu, J. (1987) Gold deposits in Precambrian iron-bearing formations-a case study of the Dongfenshan gold deposits in Heilongshang Province. *Dizhi Xuebao (Acta Geolog. Sinica)*, **61**, 58–71.

Maresch, W.V. and Czank, M. (1988) Crystal chemistry, growth kinetics and phase relationships of structurally disordered (Mn^{2+},Mg)-amphiboles. *Fortschr. Mineral.*, **66**, 69–121.

Maresch, W.V. and Mottana, A. (1976) The pyroxmangite-rhodonite transformation for the $MnSiO_3$ composition. *Contrib. Mineral. Petrol.*, **55**, 69–79.

McSwiggen, P.L., Morey, G.B. and Cleland, J.M. (1994) Occurrence and genetic implications of hyalophane in manganese-rich iron-formation, Cuyuna Iron Range, Minnesota, USA. *Mineral. Mag.*, **58**, 387–99.

Melcher, F. (1991) Fe-Ti-oxide assemblages in the basal parts of the Central Alpine Brenner Mesozoic, Tyrol/Austria. *Mineral. Petrol.*, **44**, 197–212.

Melcher, F. (1993) *Gold mineralization in Birimian (Lower Proterozoic) greenstone belts of northern Ghana: the significance of chemical sediments*. Ph.D. thesis (unpublished), 304 pp., Mining University, Leoben.

Melcher, F. and Stumpfl, E.F. (1992) Chemical facies and gold mineralization in northern Ghana. *Berichte zur Lagerstätten- und Rohstofforschung*, **13**, 233 pp., 51 Fig., 23 Tab., 37 p. Appendices.

Melcher, F. and Stumpfl, E.F. (1993) Chemical facies and gold mineralization in northern Ghana. *Z. Angew. Geol.*, **39**, 43–6.

Melcher, F. and Stumpfl, E.F. (1994) Paleoproterozoic exhalite formation in northern Ghana: Source of epigenetic gold-quartz vein mineralization? *Geol. Jahrb.*, **D100**, 201–46, Hannover.

Milési, J.P., Feybesse, J.L., Ledru, P., Dommanget, A., Quedrago, M.F., Marcoux, E., Prost, A., Vinchon, C., Sylvain, J.P., Johan, V., Tegyey, M., Calvez, J.P. and Lagny, Ph. (1989) West African gold deposits in their Lower Proterozoic lithostructural setting. *Chron. rech. min. Fr.*, **497**, 3–98, Orleáns.

Miyano, T. and Klein, C. (1989) Phase equilibria in the system K_2O–FeO–MgO–Al_2O_3–SiO_2–H_2O–CO_2 and the stability limit of stilpnomelane in metamorphosed Precambrian iron-formations. *Contrib. Mineral. Petrol.*, **102**, 478–91.

Mogessie, A. and Tessadri, R. (1982) A BASIC computer program to determine the name of an amphibole from an electron microprobe analysis. *Geol. Paläontol. Mitt. Innsbruck*, **11**, 259–89.

Mogessie, A., Tessadri, R. and Veltman, C.B. (1990) EMP-Amph- a Hypercard program to determine the name of an amphibole from electron microprobe analysis according to the International Mineralogical Association Scheme. *Computers & Geosci.*, **16**, 309–30.

Mosier, D.L. and Page, N.J. (1988) Descriptive and grade-tonnage models of volcanogenic manganese deposits in oceanic environments-a modification. *U.S. Geol. Surv. Bull.*, **1811**, 28 pp.

Mücke, A. and Bhadra Chaudhuri, J.N. (1991) The continuous alteration of ilmenite through pseudorutile to leucoxene. *Ore Geol. Rev.*, **6**, 25–44.

Mücke, A. and Okujeni, C. (1984) Geological and ore microscopic evidence on the epigenetic origin of the manganese occurrences in northern Nigeria. *J. Afr. Earth Sci.*, **2**, 209–25.

Neumann, U. (1988) *Mineralogie und Genese der Manganvorkommen in den Schiefergürteln von Nord-Nigeria*. Ph.D. thesis (unpublished), 227 pp., Universität Göttingen.

Oen, I.S., De Maesschalck, A.A. and Lustenhouwer, W.J. (1986) Mid-Proterozoic exhalative-sedimentary

Mn skarns containing possible microbial fossils, Grythyttan, Bergslagen, Sweden. *Econ. Geol.*, **81**, 1533–43.

Ostwald, J. (1988) Mineralogy of the Groote Eylandt manganese oxides: a review. *Ore Geol. Rev.*, **4**, 3–45.

Pan, Y. and Fleet, M.E. (1993) Mineralogy and genesis of calc-silicates associated with Archean volcanogenic massive sulfide deposits at the Manitouwadge mining camp, Ontario. *Can. J. Earth Sci.*, **29**, 1375–88.

Perseil, E.A. and Grandin, G. (1978) Evolution minéralogique du manganèse dans trois gisements d'Afrique de l'Ouest: Mokta, Tambao, Nsuta. *Mineral. Deposita*, **13**, 295–311.

Peters, Tj., Valarelli, J.V. Coutinho, J. M. V., Sommerauer, J. and Raumer, J. V. (1977) The manganese deposits of Buritirama (Pará, Brazil). *Schweiz. mineral. petrogr. Mitt.*, **57**, 313–27.

Petters, S.W. (1991) Regional Geology of Africa. *Lecture Notes in Earth Sciences*, **40**, 722 pp., Springer-Verlag.

Pownceby, M.I., Wall, V.J. and O'Neill, H.St.C. (1987) Fe-Mn partitioning between garnet and ilmenite: experimental calibration and applications. *Contrib. Mineral. Petrol.*, **97**, 116–26.

Robertson, A.H.F. and Hudson, J.D. (1973) Cyprus umbers: Chemical precipitates on a Tethyan ocean ridge. *Earth Planet. Sci. Let.*, **18**, 93–101.

Robinson, P., Spear, F.S., Schumacher, J.C., Laird, J., Klein, C., Evans, B.W. and Doolan, B.L. (1982) Phase relations of metamorphic amphiboles: natural occurrence and theory. *Reviews in Mineral.*, **9B**, 1–227.

Roudakov, V.M. (1965) Report on the geology and minerals of the north-western part of the Wa field sheet. *Ghana Geol. Survey Dept., Archive Report*, **50**, 95 pp. Published by Minerals Commission/GTZ Publication Project, Accra, Ghana, 1991.

Roy, S. (1965) Comparative study of the metamorphosed manganese protores of the world — the problem of the nomenclature of the gondites and kodurites. *Econ. Geol.*, **60**, 1238–60.

Roy, S. (1968) Mineralogy of the different genetic types of manganese deposits. *Econ. Geol.*, **63**, 760–86.

Roy, S. (1973) Genetic studies on the Precambrian manganese formations of India with particular reference to the effects of metamorphism. *UNESCO, Earth Science Series*, **9**, 229–42.

Roy, S. (1974) Manganese-bearing silicate minerals from metamorphosed manganese formations of India. III Tirodite. *Acta Mineralogica-Petrographica*, **21**, 269–73, Szeged, Hungaria.

Roy, S. (1981) *Manganese deposits*. Academic Press, London, 458 pp.

Roy, S. and Purkait, P.K. (1968) Mineralogy and genesis of the metamorphosed manganese silicate rocks (gondite) of Gowari Wadhona, Madhya Pradesh, India. *Contrib. Mineral. Petrol.*, **20**, 86–114.

Roy, S., Bandopadhyay, P.C., Perseil, E.A. and Fukuoka, M. (1990) Late diagenetic changes in manganese ores of the Upper Proterozoic Penganga Group, India. *Ore Geol. Rev.*, **5**, 341–57.

Rozendaal, A. and Stumpfl, E.F. (1984) Mineral chemistry and genesis of the Gamsberg zinc deposit, South Africa. *Trans. Instn. Min. Metall. (Section B: Appl. Earth Sci.)*, **93**, 161–75.

Segeler, C.G. (1961) First U.S. occurrence of manganoan cummingtonite, tirodite. *Amer. Mineral.*, **46**, 637–41.

Sivaprakash, C. (1980) Mineralogy of manganese deposits of Koduru and Garbham, Andhra Pradesh, India. *Econ. Geol.*, **75**, 1083–104.

Slack, J.F., Palmer, M.R., Stevens, B.P.J., and Barnes, R.G. (1993) Origin and significance of tourmaline-rich rocks in the Broken Hill District, Australia. *Econ. Geol.*, **88**, 505–41.

Sorem, R.K. and Cameron, E.N. (1960) Manganese oxides and associated minerals of the Nsuta manganese deposits, Ghana, West Africa. *Econ. Geol.*, **55**, 278–310.

Spry, P.G. and Wonder, J.D. (1989) Manganese-rich garnet rocks associated with the Broken Hill lead-zinc-silver deposit, New South Wales, Australia. *Can. Mineral.*, **27**, 275–92.

Sylvester, P.J. and Attoh, K. (1992) Lithostratigraphy and composition of 2.1 Ga greenstone belts of the West African craton and their bearing on crustal evolution and the Archean–Proterozoic boundary. *J. Geol.*, **100**, 377–93.

Taylor, P.N., Moorbath, S., Leube, A. and Hirdes, W. (1992) Early Proterozoic crustal evolution in the Birimian of Ghana: constraints from geochronology and isotope geochemistry. *Prec. Res.*, **56**, 97–111.

Toth, J.R. (1980) Deposition of submarine crusts rich in manganese and iron. *Geol. Soc. Amer. Bull.*, **91**, p. 44–54.

Viswanathan, K. and Kielhorn, H.M. (1983) Variations in the chemical composition and lattice dimensions of (Ba,K,Na)-feldspars from Otjosondu, Namibia and their significance. *Amer. Mineral.*, **68**, 112–21.

Winkler, H.G.F. (1974) *Petrogenesis of metamorphic rocks*. 3rd edition, Springer-Verlag, New York, 320 pp.

Winter, G.A., Essene, E.J. and Peacor, D.R. (1981) Carbonates and pyroxenoids from the manganese deposit near Bald Knob, North Carolina. *Amer. Mineral.*, **66**, 278–89.

Wonder, J.D., Spry, P.G. and Windom, K.E. (1988) Geochemistry and origin of manganese-rich rocks related to iron-formation and sulfide deposits, Western Georgia. *Econ. Geol.*, **83**, 1070–81.

Worthing, M.A. (1987) Deerite from Papua New Guinea. *Mineral. Mag.*, **51**, 689–93.

[*Manuscript received 17 February 1994: revised 10 June 1994*]